Phase behavior and structure of Janus fluids

Thorsten Erdmann,[1,2,*] Martin Kröger,[2,3] and Siegfried Hess[2]
[1]*Abteilung Theorie, Max-Planck-Institut für Kolloid- und Grenzflächenforschung, D-14424 Potsdam, Germany*
[2]*Institut für Theoretische Physik, Technische Universität Berlin, Hardenbergstrasse 36, D-10623 Berlin, Germany*
[3]*Polymer Physics, Material Sciences, ETH Zürich, CH-8092 Zürich, Switzerland*
(Received 9 October 2002; published 29 April 2003)

The equilibrium phase behavior of Janus fluids is examined based on a model potential for the interaction between their constituents. Janus fluids consist of axisymmetric particles possessing two different ''faces,'' e.g., one hydrophobic and one hydrophilic surface, and the interaction depends on the relative orientation. Starting from a short range, isotropic potential we make an ansatz for an anisotropic model interaction potential. Two types of symmetries of the particles are considered. One leads to a polar phase. The Helmholtz free energy and the pressure are calculated by the help of an augmented van der Waals approximation. A qualitative phase diagram is obtained. The appearance of a polar phase and the corresponding transition temperature are examined adapting a Landau–de Gennes expansion of the orientational part of the free energy. Monte Carlo simulations are performed and the results are compared with the ones obtained by the analytical description.

DOI: 10.1103/PhysRevE.67.041209 PACS number(s): 61.20.Gy, 61.25.−f, 61.20.Ja, 64.30.+t

I. INTRODUCTION

A macrofluid composed of particles whose interaction possesses a particular type of anisotropy was studied by Casagrande *et al.* [1]. They chemically treated glass spheres of some micrometers in diameter in such a way that one-half of the spherical surface became hydrophilic whereas the other remained hydrophobic. These amphiphilic solid ''particles'' were called ''Janus beads'' due to their spherical shape but nonspherical properties. Since then there has been great effort to reduce the size of the Janus beads by synthesizing ''Janus micelles,'' i.e., amphiphilic spheres with both hydrophilic and hydrophobic halves [2,3]. The Janus micelles synthesized so far are built of block copolymers containing separated polar and nonpolar compounds, forming the different surfaces of the molecules. They are estimated to have a diameter of about 10–20 nm and a molecular weight of about 2×10^7 g/mol [4]. For a discussion of intermolecular forces, see [5]. Experimentally, the Janus micelles need to be immersed in a suitable liquid solvent for the different building blocks, whereas in the model to be described below, the solvent is not taken into account. The sole components of the model Janus fluid are Janus particles. In this article we consider them to be effectively axisymmetric particles without head-tail symmetry, and of homogeneous mass density. Substructures and chemical details are therefore disregarded. Concerning the analytical description, the Janus fluid is treated as a macrofluid. Concerning applications, the chemical composition and the properties of amphiphilic molecules influence the parameters of the model to be described below. Two types of preferred symmetries of the particles are considered, to be denoted as ''ee'' and ''nn'' symmetries (see Fig. 1). These symmetries are different from the one which characterizes the usual dipolar fluids, denoted as ''sn'' symmetry in Fig. 1. The symmetry ee potentially leads to a polar phase, whereas the symmetry nn may possess a nematic and microphase-separated phase. The possible polar phase of a Janus fluid is defined such that the particle orientations are preferably aligned *parallel* rather than *antiparallel* to the oriented director of the fluid. Vector properties of the molecules, like electric or magnetic dipole moments, could be transferred to the whole fluid. This is in contrast to the usual nematics, where the particles are oriented along both directions of the director with equal probability, due to the tensorial character of the alignment in the nematic phase, which results from the head-tail symmetry of nematic liquid crystalline molecules and which Janus particles do not possess.

This article is organized as follows. In Sec. II the nonspherical model potential for Janus spheres is introduced. An approximation for the free energy of the fluid, starting out from an augmented van der Waals approximation [6] is derived in Sec. III. Results for the pressure of the fluid, the transition temperature into a polar phase, and the order parameters in the polar phase are presented in Sec. IV by making use of a high temperature approximation. Here, we also present a qualitative phase diagram and discuss the range of validity of—and possible corrections to—the analytical expressions. Section V is dedicated to Monte Carlo simulation of the Janus fluid. Numerical results for the pressure, order parameters, and transition temperature are compared with the

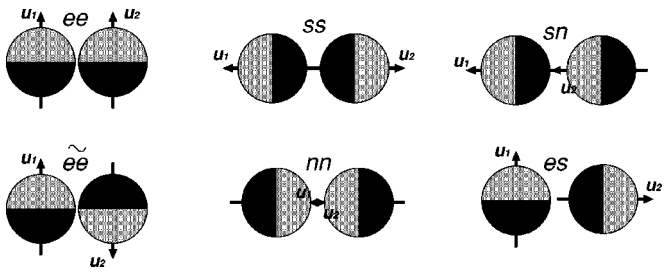

FIG. 1. Schematic representation, including nomenclature, of the basic configurations for the Janus spheres.

*Corresponding author. Electronic address: erdmann@physik.tu-berlin.de

analytic results of Sec. IV. Whereas analytically only a polar phase is considered, in the simulations other anisotropic phases were also examined, namely, a nematiclike phase.

II. THE MODEL

A. Janus spheres and binary potential function

The fluid considered in this work is composed of Janus spheres. These are effectively axisymmetric particles of spherical shape, which are composed of two different hemispheres. The energy ϕ for the binary interaction between two Janus spheres, characterized by their orientations $\mathbf{u}_1,\mathbf{u}_2$ (unit vectors) and the distance $\mathbf{r}$ between their centers can be written as a sum of its isotropic ϕ^{sph} and anisotropic ϕ^{aniso} contributions, i.e., $\phi(\mathbf{r},\mathbf{u}_1,\mathbf{u}_2)\equiv\phi^{\mathrm{sph}}(r)+\phi^{\mathrm{aniso}}(\mathbf{r},\mathbf{u}_1,\mathbf{u}_2)$, where $r\equiv|\mathbf{r}|$. The radially symmetric part ϕ^{sph} describes the average interaction between two randomly oriented Janus spheres, such that the unconditional orientational average over all directions $\mathbf{u}_1$, $\mathbf{u}_2$ vanishes for the anisotropic part ϕ^{aniso}, i.e., $\langle\langle\phi^{\mathrm{aniso}}(\mathbf{r},\mathbf{u}_1,\mathbf{u}_2)\rangle\rangle_{\rho_0}=0$, where $\langle\langle\cdots\rangle\rangle_\rho \equiv\int\int\cdots\rho(\mathbf{u}_1)\rho(\mathbf{u}_2)d^2u_1d^2u_2$ stands for an average by means of the single particle orientational distribution function $\rho(\mathbf{u})$, normalized such that $1=\langle\langle 1\rangle\rangle_\rho$. The condition for ϕ^{aniso} involves the homogeneous (random) orientational distribution function $\rho_0=(4\pi)^{-1}$.

Here, the radially symmetric part of the potential ϕ is modeled by the SHRAT (short range attractive) potential introduced in [7] and [8]. It has a repulsive core and an attractive well with a smooth cutoff at finite distance and possesses a relatively simple functional form. The SHRAT potential is written as the sum of a positive and a negative part, i.e., $\phi^{\mathrm{sph}}=\phi^{\mathrm{SHRAT}}$ with

$$\phi^{\mathrm{SHRAT}}(r)=\frac{256}{27}\phi_0[(3-2r^*)^4-(3-2r^*)^3] \qquad (1)$$

for $r^*\equiv r/r_0\leqslant 1.5$, and $\phi=0$ otherwise [7]. The parameters r_0 and ϕ_0 set the characteristic length and energy scales. Together with the mass m of a Janus sphere, the three quantities are used to express all quantities in terms of dimensionless units marked by an asterisk. For any measurable quantity Q with a dimension specified in SI units kg, m and s one has $Q=Q^*Q_{\mathrm{ref}}$ and $Q_{\mathrm{ref}}=m^{\alpha+\gamma/2}r_0^{\beta+\gamma}\phi_0^{-\gamma/2}$, for $[Q]=\mathrm{kg}^\alpha\ \mathrm{m}^\beta\ \mathrm{s}^\gamma$. The reference values for length r, number density n, energy k_BT, and pressure p are therefore $r_{\mathrm{ref}}=r_0$, $n_{\mathrm{ref}}=r_0^{-3}$, $E_{\mathrm{ref}}=\phi_0=k_BT_{\mathrm{ref}}$, and $p_{\mathrm{ref}}=\phi_0r_0^{-3}=n_{\mathrm{ref}}E_{\mathrm{ref}}$. In all figures throughout this article dimensionless quantities Q^* are shown. Unlike the often used Lennard-Jones (LJ) potential [9] the SHRAT potential is finite for vanishing distance. Due to the small value of the Boltzmann factor $\exp\{-\beta\phi^{\mathrm{SHRAT}}(r=0)\}\leqslant 6\times10^{-23}$, with $\beta\equiv 1/k_BT$ for thermal energies $T^*=k_BT/\phi_0\leqslant 10.0$ essentially no particle of the fluid has enough energy to reach $r=0$. Note, that for convenience in the following T stands for the dimensionless temperature T^*, whenever it comes *without* Boltzmann's constant k_B. In the form (1), with the special choice $r^*_{\mathrm{cut}}=1.5$ for the cutoff distance, the SHRAT potential resembles the LJ potential insofar as the equilibrium (or minimum) distance $r^*_{\mathrm{eq}}=9/8=1.125$ is almost equal to the LJ equilibrium distance $r^{\mathrm{LJ},*}_{\mathrm{eq}}=2^{1/6}\approx 1.122$, the potential well depth is $\phi^*(r_{\mathrm{eq}})=1$ for both functions, and the derivatives $(\partial\phi/\partial r)(r_0)$ of the functions at distance r_0, where they are at least comparable.

For the anisotropic part ϕ^{aniso} the ansatz

$$\phi^{\mathrm{aniso}}(\mathbf{r},\mathbf{u}_1,\mathbf{u}_2)=-(256/27)\,\phi_0(3-2r^*)^3\psi(\hat{\mathbf{r}},\mathbf{u}_1,\mathbf{u}_2) \qquad (2)$$

for $r^*\leqslant 1.5$, and $\phi^{\mathrm{aniso}}=0$ otherwise, is chosen. This means that the nonspherical potential function ϕ can be considered as a SHRAT potential with a nonspherical negative part. The anisotropy of this ansatz is described by the anisotropy function $\psi(\hat{\mathbf{r}},\mathbf{u}_1,\mathbf{u}_2)$, depending on the unit vectors $\mathbf{u}_1$, $\mathbf{u}_2$ and $\hat{\mathbf{r}}=\mathbf{r}/r$.

The dependence on these unit vectors is taken into account using symmetric, irreducible (anisotropic) Cartesian tensors, also referred to as spherical harmonic tensors. Such an anisotropic tensor of rank ℓ constructed from a given unit vector $\mathbf{u}=(u_1,u_2,u_3)$ has the form

$$\varphi_{\mu_1\cdots\mu_\ell}(\mathbf{u})\equiv\sqrt{\frac{(2\ell+1)!!}{\ell!}}\,\overline{u_{\mu_1}\cdots u_{\mu_\ell}}, \qquad (3)$$

where the symbol

$$\overline{u_{\mu_1}\cdots u}_{\mu_\ell}$$

indicates the symmetric irreducible part of the ℓ-fold dyadic product of $\mathbf{u}$, and $\mu_1,\mu_2,..\in\{1,2,3\}$ denote Cartesian indices. The normalization coefficients are chosen such that the "square" of a tensor of rank ℓ is $2\ell+1$, e.g., $\varphi_\mu(\mathbf{u})\varphi_\mu(\mathbf{u})=3$. The summation convention for repeated indices is used. The tensors (3) are directly related to the spherical harmonic functions Y^μ_λ [10]. The first and second rank Cartesian tensors (3) explicitly read

$$\varphi_\mu(\mathbf{u})=\sqrt{3}u_\mu,$$

and

$$\varphi_{\mu\nu}(\mathbf{u})=(15/2)^{1/2}\,\overline{\mathbf{uu}}_{\mu\nu}=(15/2)^{1/2}\,(u_\mu u_\nu-\delta_{\mu\nu}/3).$$

The scalar function $\psi(\hat{\mathbf{r}},\mathbf{u}_1,\mathbf{u}_2)$ characterizing the anisotropy of the energy remains to be specified. We assume a linear combination of terms constructed from these first and second rank tensors upon contraction which is compatible with (i) the symmetry of the Janus spheres and their shape, (ii) the invariance against exchanging particles 1 and 2, and (iii) the condition $\langle\langle\phi^{\mathrm{aniso}}\rangle\rangle_{\rho_0}=0$. According to these assumptions the anisotropy function $\psi=\psi(\hat{\mathbf{r}},\mathbf{u}_1,\mathbf{u}_2)$ contains three independent parameters $\varepsilon_{1,2,3}$ and reads

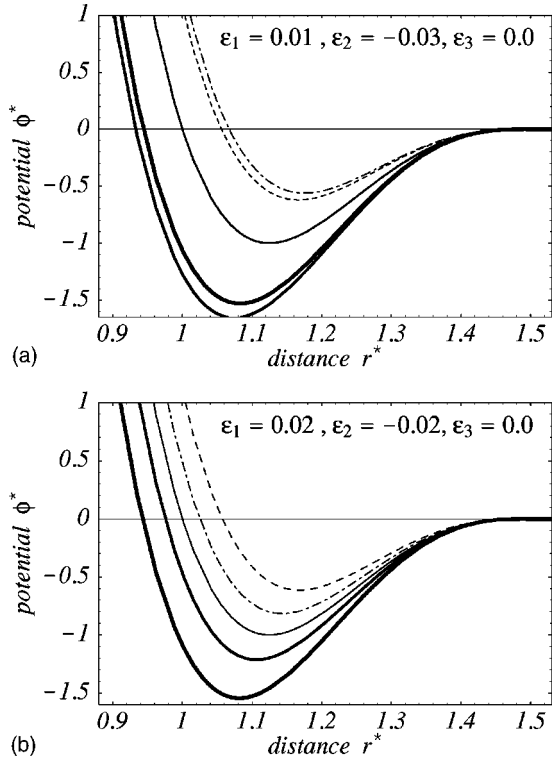

FIG. 2. The potential functions $\phi_{ee}(r)$ (thick curve), $\phi_{nn}(r)$ (slightly thinner curve), $\phi_{sn}(r)$ (dash-dotted curve), $\phi_{\widetilde{ee}}(r)$ (dashed curve), together with the isotropic SHRAT potential (thin curve) in the middle, with $\varepsilon_3=0$ and the values $\varepsilon_1=0.01$, $\varepsilon_2=-0.03$ (top) and $\varepsilon_1=0.02$, $\varepsilon_2=-0.02$ (bottom) of the two other anisotropy parameters.

$$\psi=\varepsilon_1\varphi_\mu(\mathbf{u}_1)\varphi_\mu(\mathbf{u}_2)+\varepsilon_2\varphi_\mu(\mathbf{u}_1)\varphi_{\mu\nu}(\hat{\mathbf{r}})\varphi_\nu(\mathbf{u}_2)$$
$$+\varepsilon_3[\varphi_\mu(\mathbf{u}_1)\varphi_\mu(\hat{\mathbf{r}})-\varphi_\mu(\mathbf{u}_2)\varphi_\mu(\hat{\mathbf{r}})]$$
$$=3\varepsilon_1\mathbf{u}_1\cdot\mathbf{u}_2+3\varepsilon_3(\mathbf{u}_1\cdot\hat{\mathbf{r}}-\mathbf{u}_2\cdot\hat{\mathbf{r}})+\varepsilon_2(135/2)^{1/2}$$
$$\times[(\mathbf{u}_1\cdot\hat{\mathbf{r}})(\mathbf{u}_2\cdot\hat{\mathbf{r}})-\mathbf{u}_1\cdot\mathbf{u}_2/3]. \quad (4)$$

Tensors of second rank and terms of second order in the axes vectors $\mathbf{u}_1$ and $\mathbf{u}_2$, as needed for nematics, are disregarded in this expression due to the symmetry and shape of the particles. The three coefficients $\varepsilon_{1,2,3}$ are referred to as the anisotropy coefficients and allow one to characterize the particle interaction of Janus type. Similar expansions were applied in the kinetic theory and the scattering of rotating molecules (see [11]). The term involving ε_2 has an angle dependence corresponding to that of an electric or magnetic dipole-dipole interaction, where $\varepsilon_2>0$ for identical dipoles. A specific case with $\varepsilon_2<0$ had been studied in [12]. The scalar functions (rotational invariants) in expression (4) are some of the S functions, namely, $S_{110}(\mathbf{u}_1,\mathbf{u}_2,\hat{\mathbf{r}})$, $S_{112}(\mathbf{u}_1,\mathbf{u}_2,\hat{\mathbf{r}})$ and $S_{101}(\mathbf{u}_1,\mathbf{u}_2,\hat{\mathbf{r}})-S_{011}(\mathbf{u}_1,\mathbf{u}_2,\hat{\mathbf{r}})$. Stone [13] used these for a general expansion of functions of three unit vectors. Expansion (4) is a special case of such a general expansion for a nonspherical function, restricted to the lowest order rotational invariant compatible with the symmetry of the Janus spheres.

TABLE I. The table collects the effect of choice of parameters $\varepsilon_{1,2,3}$—positive (+), zero (0), negative (−)—on the possibly preferred (●) and unpreferred (○) configurations (cf. Fig. 1), with lowest energy. Cases where $\varepsilon_{1,2}=0$ are not tabulated. If more than a single phase is possible, the preferred one depends on the explicit values for the parameters. The en phase may be stable for $\varepsilon_2=0$, $\varepsilon_{1,3}>0$. The case +, −, 0 is the one mostly considered in this work. Here, the nn phase is stable for $0<\varepsilon_1\leqslant-(5/24)^{1/2}\varepsilon_2$; otherwise the ee phase is preferred.

ε_1	+	+	+	+	+	+	-	-	-	-	-	-
ε_2	+	+	+	-	-	-	+	+	+	-	-	-
ε_3	+	-	0	+	-	0	+	-	0	+	-	0
nn	○	●	○	○	●	●	○	●	○	○	●	●
ss	●	○	○	●	○	●	●	○	○	●	○	●
sn	●	●	●	○	○	○	●	●	●	○	○	○
ee	○	○	○	●	●	●	○	○	○	○	○	○
$\widetilde{\text{ee}}$	○	○	○	○	○	○	●	●	●	○	○	○
es	○	○	○	○	○	○	○	○	○	○	○	○
en	○	○	○	○	○	○	○	○	○	○	○	○

B. Discussion of the potential

To elucidate the physical meaning of the anisotropy of the potential function and the influence of the anisotropy parameters, it is useful to examine the nonspherical potential function ϕ for fixed relative position and fixed axes of the interacting particles in some characteristic ''basic configurations.'' The potential function is then a mere function of the distance r of the particles. The basic configurations considered here are the (i) nn configuration (ss configuration) with $\hat{\mathbf{r}}=\mathbf{u}_1=-\mathbf{u}_2$, i.e., the particles point with their ''north poles'' (''south poles'') toward each other; (ii) sn configuration with $\mathbf{u}_1=\mathbf{u}_2=\pm\hat{\mathbf{r}}$, i.e., one particle points with its ''north pole'' to the ''south pole'' of the other; (iii) ee configuration ($\widetilde{\text{ee}}$ configuration) with $\hat{\mathbf{r}}\perp\mathbf{u}_1=\pm\mathbf{u}_2$, i.e., the particles are parallel (antiparallel) to each other with their ''equators'' touching each other; (iv) es and en configuration with $\mathbf{u}_1\perp\mathbf{u}_2=\pm\hat{\mathbf{r}}$, i.e., one particle points with its ''north pole'' (''south pole'') toward the ''equator'' of the other. These basic configurations are sketched in Fig. 1. For the different basic configurations, the anisotropy function $\psi(\hat{\mathbf{r}},\mathbf{u}_1,\mathbf{u}_2)$ is $\psi_{\text{nn}}=-3\varepsilon_1-30^{1/2}\,\varepsilon_2-6\varepsilon_3$, $\psi_{\text{ss}}=-3\varepsilon_1-30^{1/2}\,\varepsilon_2+6\varepsilon_3$, $\psi_{\text{sn}}=3\varepsilon_1+30^{1/2}\,\varepsilon_2$, $\psi_{\text{ee}}=3\varepsilon_1-(15/2)^{1/2}\,\varepsilon_2$, $\psi_{\widetilde{\text{ee}}}=-3\varepsilon_1+(15/2)^{1/2}\,\varepsilon_2$, $\psi_{\text{es}}=-3\varepsilon_3$, $\psi_{\text{en}}=3\varepsilon_3$. The potential curves for some of the basic configurations are plotted in Fig. 2 for two different sets of anisotropy parameters. For both sets, the ee and nn configurations are energetically favored, i.e., the potential energy is reduced with respect to the SHRAT potential for all distances. This should be the case for amphiphilic particles with an additional attraction between identical halves. It turns out that not only are the values of the potential curves reduced, but also the minimum distance r_{eq} is shifted according to $r^*_{\text{eq}}=1/(1+\psi)$ for $\psi>-1$, as is the zero of the potential function. For a more exhaustive summary on the characteristics of the potential see Table I.

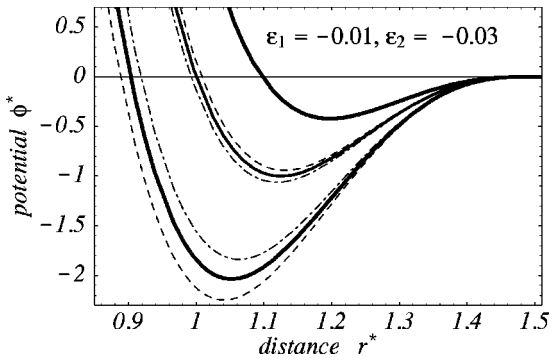

FIG. 3. The lower group of lines represents the potential functions $\phi_{nn}(\varepsilon_1=-0.01,\ \varepsilon_2=-0.03,\ \varepsilon_3=0.005)$ (dash-dotted curve), ϕ_{ss} $(-0.01,-0.03,\ 0.005)$ (dashed curve), and $\phi_{nn}(-0.01,\ -0.03,\ 0.0)$ (thick curve); the uppermost solid curve shows $\phi_{sn}(-0.01,-0.03)$. The group of curves in the middle shows the SHRAT potential ϕ^{SHRAT} (solid curve), $\phi_{en}(\varepsilon_3=0.005)$ (dash-dotted curve), and $\phi_{es}(0.005)=\phi_{en}(-0.005)$ (dashed curve).

The two sets characterize the two important variations of Janus fluids. The first set corresponds to proper Janus spheres where the nn configuration has the lowest energy (nn Janus spheres). The second set, where the ee configuration is favored, can lead to phases with dipolar symmetry in analogy to phases observed for systems composed of pear shaped molecules, which also give rise to flexoelectric effects [14]. These particles may be called Janus dipoles (or ee Janus spheres). The tendency to prefer the nn configuration with respect to the ee configuration is stronger for negative values of ε_1. Table I gives an overview of the preferred configurations for positive and negative values of the different anisotropy parameters. In the following we refer to both types of particles as Janus spheres. The term involving ε_2 has an angle dependence corresponding to that of an electric or magnetic dipole-dipole interaction, where $\varepsilon_2>0$ for identical dipoles. A particular case with $\varepsilon_2<0$ had been elaborated in [12]. The third parameter ε_3 appears only in ψ for the basic configuration, for which reversing the directions of both particle axes simultaneously yields a different, though related configuration, as is the case for ee and $\widetilde{\mathrm{ee}}$ or nn and ss. Thus, ε_3 describes a difference in the strength of interaction between ''black'' and ''gray'' halves—north and south poles—of the particles. In the following, this difference will usually be neglected and ε_3 will be set to zero. Only sporadically nonzero values of ε_3 will be considered to highlight its influence on certain physical quantities. Figure 3 shows its influence on the potential functions in the basic configurations.

III. FREE ENERGY AND PRESSURE OF A JANUS FLUID

A. The different contributions to the free energy

Classically, the free energy per particle $f(n,T)=F(N,V,T)/N$ of a fluid composed of nonspherical Janus spheres is written as the sum $f(n,T)=f_{\mathrm{kin}}(n,T)+f_{\mathrm{pot}}(n,T)+f_{\mathrm{or}}(T)$, of a kinetic, a potential, and an entropic contribution. The latter is associated with the orientation of the particle axes. In the above, N designates the number of particles in the fluid, V its volume, and T its temperature. $n=N/V$ is the number density of the fluid. From the free energy per particle, the pressure of the fluid is obtained through the derivative with respect to density: $p(n,T)=n^2(\partial f(n,T)/\partial n)_T$.

(*a*) *The kinetic contribution* f_{kin} also referred to as the ideal gas contribution, is

$$f_{\mathrm{kin}}(n,T)=k_{\mathrm{B}}T[\ln(n\lambda^3)-1]=f_{\mathrm{ideal}}(n,T), \tag{5}$$

with the thermal de Broglie wavelength $\lambda=(mk_{\mathrm{B}}T/\hbar)^{-1/2}$. $\hbar$ is Planck's constant and m the mass of a particle.

(*b*) *The entropic contribution* f_{or} stems from an alignment of the nonspherical particles of the fluid. Here we assume that it is represented by the statistical entropy

$$f_{\mathrm{or}}(T)=k_{\mathrm{B}}T\langle\ln(\rho(\mathbf{u})/\rho_0)\rangle_\rho, \tag{6}$$

where $\langle\cdots\rangle_\rho\equiv\int\cdots\rho(\mathbf{u})d^2u$ denotes an orientational average with ρ. The orientational free energy vanishes for isotropic alignment, $\rho=\rho_0=(4\pi)^{-1}$. It had been used, e.g., by Onsager for the description of long rods [15]. The use of the *single* particle distribution function neglects all correlations between two and more particles and is therefore a potential candidate for future improvements of the model. The kinetic part of the pressure $p_{\mathrm{kin}}=nk_{\mathrm{B}}T$ is the usual ideal gas pressure. There is no entropic contribution because Eq. (6) does not depend on the density.

(*c*) *The potential contribution* f_{pot} is taken into account by an augmented van der Waals approximation. The augmented van der Waals approximation was introduced in [6] and applied to a spherical LJ fluid. The agreement with numerical data for the pressure was fairly good. In [20] it was also applied to a fluid with nonspherical interaction potential. This approximation decomposes the potential contribution $f_{\mathrm{pot}}(n,T)$ to the free energy into the contribution $f_{\mathrm{rep}}(n,T)$ of a purely repulsive, spherical potential $\phi^{\mathrm{rep}}(r)$ and a contribution $f_{\mathrm{dis}}(n,T)$ of a distortion potential $\phi^{\mathrm{dis}}(\hat{\mathbf{r}},\mathbf{u}_1,\mathbf{u}_2)=\phi(\hat{\mathbf{r}},\mathbf{u}_1,\mathbf{u}_2)-\phi^{\mathrm{rep}}(r)$, i.e., $f_{\mathrm{pot}}=f_{\mathrm{rep}}+f_{\mathrm{dis}}$. The nonspherical or nonrepulsive parts are referred to as the distortion part, because in a dense fluid the radially symmetric repulsive forces usually give the major contribution to the free energy [16].

(*d*) *The radially symmetric repulsive contribution.* In analogy to the Weeks-Chandler-Andersen (WCA) potential [17] which is the repulsive part of the LJ potential, the SHRAT potential truncated at its minimum and shifted such that it vanishes continuously is used as the spherical, purely repulsive potential: $\phi^{\mathrm{rep}}(r)=\phi^{\mathrm{SHRAT}}(r)+\phi_0$ for $r\leqslant r_{\mathrm{eq}}$, and $\phi^{\mathrm{SHRAT}}=0$ otherwise, with $r^*_{\mathrm{eq}}=9/8$. Its contribution to the free energy is calculated with a modified Carnahan-Starling expression. The Carnahan-Starling expression f_{CS} for the free energy—originally derived in [18] for a fluid of hard spheres—is $\beta f_{\mathrm{CS}}(n,T)=nB_2^{\mathrm{hs}}/(1-nv)+(nv)^2/(1-nv)^2$, where $B_2^{\mathrm{hs}}=4v$ is the second virial coefficient for the hard sphere potential, v denotes the volume of a hard sphere, and $\beta\equiv 1/k_{\mathrm{B}}T$. For the application of this expression to the repulsive soft sphere potential $\phi^{\mathrm{rep}}(r)$ the second virial coeffi-

cient B^{hs} is replaced with the temperature dependent virial coefficient of the soft potential:

$$B_2^{\mathrm{rep}}(T)=\frac{1}{2}\int_{\mathbb{R}^3}1-e^{-\beta\phi^{\mathrm{rep}}(r)}d^3r, \tag{7}$$

and the volume v is replaced with an effective, temperature dependent volume $v_{\mathrm{eff}}(T)=(\pi/6)d_{\mathrm{eff}}^3(T)$. As the effective diameter $d_{\mathrm{eff}}(T)$ of a particle we use the distance where the potential energy equals the thermal energy $\phi_{\mathrm{rep}}(d_{\mathrm{eff}}(T))=k_{\mathrm{B}}T$, or equivalently, $\phi_{\mathrm{rep}}^*(d_{\mathrm{eff}})=T$. For the WCA potential this leads to $v_{\mathrm{eff}}^*(T)=(\pi/6)2^{1/2}(1+T)^{-1/4}$. We will adopt this simple expression for the present purpose, since both potentials WCA and ϕ^{rep} are very similar, and the effective volume corresponding to the WCA potential is much simpler. The modified Carnahan-Starling expression for f_{rep} then becomes

$$f_{\mathrm{rep}}(n,T)=k_{\mathrm{B}}T\left(\frac{nB_2^{\mathrm{rep}}(T)}{[1-nv_{\mathrm{eff}}(T)]}+\frac{[nv_{\mathrm{eff}}(T)]^2}{[1-nv_{\mathrm{eff}}(T)]^2}\right). \tag{8}$$

This expression was applied earlier to a WCA fluid [19,8] and yielded good agreement with results of molecular dynamics computer simulations for the corresponding pressure of the fluid.

(*e*) *The distortion contribution*

$$\phi^{\mathrm{dis}}(\hat{\mathbf{r}},\mathbf{u}_1,\mathbf{u}_2)=\phi(\hat{\mathbf{r}},\mathbf{u}_1,\mathbf{u}_2)-\phi^{\mathrm{rep}}(r)$$

of the potential includes the attractive part of the nonspherical interaction as well as the anisotropy of the repulsion, which was not included in ϕ^{rep}. The augmented van der Waals approximation takes its contributions f_{dis} to the free energy into account through the virial expression $f_{\mathrm{dis}}(n,T)=nk_{\mathrm{B}}T[B_2(T)-B_2^{\mathrm{rep}}(T)]$, and the distortion contribution to the pressure is $p_{\mathrm{dis}}(n,T)=n^2k_{\mathrm{B}}T[B_2(T)-B_2^{\mathrm{rep}}(T)]$. Here, B_2 is the second virial coefficient of the full nonspherical potential function ϕ, i.e., $B_2(T)\equiv\langle\langle B(\mathbf{u}_1\cdot\mathbf{u_2})\rangle\rangle_\rho$, and $B(\mathbf{u}_1\cdot\mathbf{u}_2)\equiv\int_{\mathbb{R}^3}1-\exp\{-\beta\phi(\mathbf{r},\mathbf{u}_1,\mathbf{u}_2)\}d^3r$. The full expression for the potential contribution to the free energy $f_{\mathrm{pot}}=f_{\mathrm{rep}}+f_{\mathrm{dis}}$ is thus obtained:

$$f_{\mathrm{pot}}(n,T)=nk_{\mathrm{B}}T\left(B_2+\frac{nv_{\mathrm{eff}}B_2^{\mathrm{rep}}}{(1-nv_{\mathrm{eff}})}+\frac{nv_{\mathrm{eff}}^2}{(1-nv_{\mathrm{eff}})^2}\right). \tag{9}$$

For high densities this expression becomes the modified Carnahan-Starling approximation, which should be a good approximation, as the repulsive part of the interaction becomes most important. For very low densities on the other hand the choice for f_{dis} guarantees that Eq. (9) becomes the virial expansion of second order and is a good approximation in this range also.

B. Isotropic and alignment free energy

Having established an expression for the free energy in terms of the orientational distribution function, density, and temperature, by making use of the augmented van der Waals approximation in the previous subsection, we want to derive conditions for the existence and stability of anisotropic phases in the Janus fluid. It is therefore necessary to decompose the free energy differently. We should denote by f_{iso} that part of the free energy which does not depend on the alignment of the particles and is the same in the isotropic and anisotropic phases of the fluid. By f_{align} we should denote that (remaining) part of the free energy that vanishes in the isotropic phase. In view of the foregoing discussion, the decomposition is already achieved for f_{kin} and f_{rep}, which are both independent of an alignment and are thus part of $f_{\mathrm{iso}}(n,T)$, and for f_{or}, which vanishes in the isotropic phase, i.e., for $\rho(\mathbf{u})=\rho_0$, and is thus part of $f_{\mathrm{align}}(n,T)$. The distortion part f_{dis} of the free energy contains isotropic as well as alignment contributions and must be further decomposed.

To proceed, the orientational distribution function is written as $\rho(\mathbf{u})=\rho_0[1+\chi(\mathbf{u})]$, with the isotropic orientational distribution function ρ_0. The function $\chi(\mathbf{u})$ with $\langle\chi(\mathbf{u})\rangle=0$ describes the anisotropy of the distribution function $\rho(\mathbf{u})$. Inserting this representation for ρ into the expression for the distortion part of the free energy f_{dis} yields

$$\begin{aligned}
f_{\mathrm{dis}}(n,T)&=f_{\mathrm{dis}}^{\mathrm{iso}}(n,T)+f_{\mathrm{dis}}^{\mathrm{aniso}}(n,T)+f_{\mathrm{dis}}^{\mathrm{align}}(n,T),\\
f_{\mathrm{dis}}^{\mathrm{iso}}(n,T)&=nk_{\mathrm{B}}T[B_2^{\mathrm{SHRAT}}(T)-B_2^{\mathrm{rep}}(T)],\\
f_{\mathrm{dis}}^{\mathrm{aniso}}(n,T)&=nk_{\mathrm{B}}TB_{2,0}^{\mathrm{aniso}}(T),\\
f_{\mathrm{dis}}^{\mathrm{align}}(n,T)&=nk_{\mathrm{B}}TH(T).
\end{aligned} \tag{10}$$

Here, the virial coefficient of a SHRAT fluid $B_2^{\mathrm{SHRAT}}(T)$ is defined in analogy to Eq. (7), and the ''virial coefficient''

$$\begin{aligned}
B_{2,0}^{\mathrm{aniso}}(T)&\equiv B_{2,0}(T)-B_2^{\mathrm{SHRAT}}(T)\\
&=\frac{1}{2}\int_{\mathbb{R}^3}\langle\langle 1-e^{-\beta\phi^{\mathrm{aniso}}}\rangle\rangle_{\rho_0}e^{-\beta\phi^{\mathrm{SHRAT}}(r)}d^3r
\end{aligned} \tag{11}$$

with $B_{2,0}(T)\equiv\langle\langle B(\mathbf{u}_1\cdot\mathbf{u}_2)\rangle\rangle_{\rho_0}$ describes the additional contribution of the *anisotropic* part ϕ^{aniso} of the potential to the free energy (and the pressure) of an *isotropic* Janus fluid. These last expressions are both independent of $\chi(\mathbf{u})$ and are thus part of the isotropic part f_{iso} of the free energy. The contribution to f_{dis} which carries the dependence on χ involves the quantity H with

$$H(T)=-\frac{1}{2}\int_{\mathbb{R}^3}\langle c_{\mathrm{aniso}}(\mathbf{r},\mathbf{u}_1,\mathbf{u}_2)\chi(\mathbf{u}_1)\chi(\mathbf{u}_2)\rangle_{\rho_0}d^3r \tag{12}$$

and the ''direct correlation function'' $c_{\mathrm{aniso}}(\mathbf{r},\mathbf{u_1},\mathbf{u_2})$, in the approximation applied here given by

$$c_{\mathrm{aniso}}=(e^{-\beta\phi^{\mathrm{aniso}}}-\langle\langle e^{-\beta\phi^{\mathrm{aniso}}}\rangle\rangle_{\rho_0})e^{-\beta\phi^{\mathrm{SHRAT}}(r)}. \tag{13}$$

The contribution $f_{\mathrm{dis}}^{\mathrm{align}}$ which carries the direct correlation function (13) is part of the alignment free energy, together with f_{or}.

The complete expression for the free energy *f*, suitable for a discussion on stability, now separates as follows:

$$f(n,T)=f_{\mathrm{iso}}(n,T)+f_{\mathrm{align}}(n,T),$$

$$f_{\mathrm{iso}}=f_{\mathrm{kin}}+f_{\mathrm{rep}}+f_{\mathrm{dis}}^{\mathrm{iso}}+f_{\mathrm{dis}}^{\mathrm{aniso}},$$

$$f_{\mathrm{align}}=f_{\mathrm{dis}}^{\mathrm{align}}+f_{\mathrm{or}}. \tag{14}$$

All contributions are explicitly defined through Eqs. (5), (6), (8), and (10), together with the definitions for a number of virial coefficients provided by Eqs. (7), (11), and (12). These coefficients involve the model potentials given in Sec. II A. The corresponding expression for the pressure reads $p(n,T)=p_{\mathrm{iso}}(n,T)+p_{\mathrm{align}}(n,T)$, $p_{\mathrm{iso}}=p_{\mathrm{kin}}+p_{\mathrm{rep}}+p_{\mathrm{dis}}^{\mathrm{iso}}+p_{\mathrm{dis}}^{\mathrm{aniso}}$, $p_{\mathrm{align}}=p_{\mathrm{dis}}^{\mathrm{align}}$. At this stage the free energy and the pressure thus depend on the single particle orientational distribution function $\rho(\mathbf{u})$ (or $\chi=4\pi\rho-1$) and three parameters $\varepsilon_{1,2,3}$ introduced in Eq. (4). Next, we should simplify the above expressions by using a multipole expansion for χ. A further simplification invokes the assumption of uniaxial alignment in Sec. III D by which the existence of a polar phase can be investigated analytically, (see Sec. IV).

C. Landau–de Gennes expansion for the alignment free energy

The existence of a stable anisotropic (polar) phase at a certain density n and temperature T requires that the alignment free energy $f_{\mathrm{align}}(n,T)$ has a minimum for an anisotropic orientational distribution function $\chi(\mathbf{u})\neq 0$ at this state point. To find these minima an expansion for f_{align} of the Landau–de Gennes type [15] is established as follows. First, the orientational distribution function $\rho=(1+\chi)\rho_0$ is written as a multipole expansion up to second order,

$$\chi(\mathbf{u})\approx a_\mu\varphi_\mu(\mathbf{u})+a_{\mu\nu}\varphi_{\mu\nu}(\mathbf{u}). \tag{15}$$

Here and in the following the summation convention is used for repeated indices. Second, the logarithm under the integral in expression (6) is expanded for small values of $\chi(\mathbf{u})$, i.e., for weak alignment, into a Taylor series of third order: $\ln(1+\chi)\approx\chi-1/2\chi^2+1/3\chi^3$ such that the entropic part becomes $f_{\mathrm{or}}\approx\langle\chi\rangle_{\rho_0}-1/2\langle\chi^2\rangle_{\rho_0}+1/3\langle\chi^3\rangle_{\rho_0}$. Due to the choice of symmetric, irreducible Cartesian basis tensors $\varphi_{\mu\ldots}$ [Eq. (3)], the coefficients $a_{\mu\ldots}$ of the expansion (15), usually denoted as alignment tensors, equal the moments of the distribution, i.e., $a_{\mu\ldots}=\langle\varphi_{\mu\ldots}(\mathbf{u})\rangle_\rho$. In a nematic liquid crystalline phase [head-tail symmetry, $\rho(\mathbf{u})=\rho(-\mathbf{u})$] the alignment tensors of odd rank vanish. For a Janus fluid, however, alignment tensors of any rank may be nonzero. A nonvanishing first rank alignment tensor a_μ (actually it is a vector with three components $a_{1,2,3}$) indicates the existence of a polar phase in the fluid.

Inserting the multipole expansion (15) into f_{align} from Eq. (14) we obtain an expansion for the alignment free energy f_{align} of a Landau–de Gennes type, if we neglect all terms including alignment tensors of rank higher than 2, and also terms containing both alignment tensors of first and second rank in at least second order:

$$\begin{aligned} f_{\mathrm{align}}(n,T)&\approx f_{\mathrm{align}}^{\mathrm{LdG}}(n,T)\\ &\equiv\frac{k_{\mathrm{B}}T}{2}\Big(A_1a_\mu a_\mu+A_2a_{\mu\nu}a_{\mu\nu}\\ &\quad-\sqrt{\frac{6}{5}}a_\mu a_\nu a_{\mu\nu}+\frac{6}{5}(a_\mu a_\mu)^2\Big). \end{aligned} \tag{16}$$

The coefficients $A_1(n,T)$ and $A_2(n,T)$ are functions of temperature and density:

$$\begin{pmatrix}A_1\\A_2\end{pmatrix}=1-n\int_{\mathbb{R}^3}\left\langle\left\langle\begin{pmatrix}\varphi_\kappa(\mathbf{u}_1)\varphi_\kappa(\mathbf{u}_2)/3\\ \varphi_{\kappa\lambda}(\mathbf{u}_1)\varphi_{\kappa\lambda}(\mathbf{u}_2)/5\end{pmatrix}c_{\mathrm{aniso}}\right\rangle\right\rangle_{\rho_0}d^3r, \tag{17}$$

where the arguments in $c_{\mathrm{aniso}}(\mathbf{r},\mathbf{u}_1,\mathbf{u}_2)$, cf. Eq. [13], have been skipped. The purely numerical coefficients in Eq. (16) result from the entropic contribution f_{or}. The effect of density on $A_{1,2}$ results from $f_{\mathrm{dis}}^{\mathrm{align}}$.

D. Uniaxial alignment

For the special case of homogeneous uniaxial alignment of particle axes, the alignment tensors can be expressed in terms of a spatial unit vector $\mathbf{n}$, the director, and scalar order parameters. The Cartesian components of the first and second order alignment tensors are

$$a_\mu=\sqrt{3}S_1n_\mu,\quad a_{\mu\nu}=\sqrt{\frac{15}{2}}S_2\overline{n_\mu n_\nu}. \tag{18}$$

The order parameters S_1 and S_2 [21] with $S_i\equiv\langle P_i(\mathbf{u}\cdot\mathbf{n})\rangle_\rho$, a director $\mathbf{n}$ defined through Eq. (18), and Legendre polynomials $P_i(i=1,2)$ characterize the polar phase and degree of alignment of the Janus fluid, respectively. Inserting the uniaxial alignment tensors into Eq. (16), the free energy associated with the alignment (16) becomes

$$f_{\mathrm{align}}^{\mathrm{LdG}}(n,T)=\frac{k_{\mathrm{B}}T}{2}\left(3(A_1-2S_2)S_1^2+\frac{54}{5}S_1^4+5A_2S_2^2\right), \tag{19}$$

and the pressure associated with the distortion part of the free energy, [see Eq. (14)], is

$$p_{\mathrm{align}}^{\mathrm{LdG}}(n,T)=\frac{nk_{\mathrm{B}}T}{2}[3(A_1-1)S_1^2+5(A_2-1)S_2^2]. \tag{20}$$

One notices, that expression (19) is even in S_1, and asymmetric in S_2. Positive (negative) values of $-1/2\leqslant S_2\leqslant 1$ describe a preferred alignment parallel (perpendicular) to the director $\mathbf{n}$, and $0\leqslant S_1\leqslant 1$ is always positive (or zero) for convenience.

E. Minima of f_{align} and order parameters

Minimizing $f_{\text{align}}^{\text{LdG}}$ [Eq. (19)] yields the equilibrium order parameters $S_{1,2}$ in terms of the coefficients $A_{1,2}(n,T)$ from Eq. (17), as follows:

$$S_1(n,T)=\sqrt{\frac{-5A_1A_2}{6(6A_2-1)}}, \tag{21a}$$

$$S_2(n,T)=-\frac{A_1/2}{6A_2-1}. \tag{21b}$$

These expressions are finite only for $A_2>1/6$ (for the temperature approaching infinity and vanishing density, one has $A_2=1$). Therefore, $A_2>0$ and expression (21b) can be real only for $A_1<0$. For high temperatures and low densities A_1 is positive, and the transition temperature T_{c} into a polar phase is determined by the condition

$$A_1(n,T_{\text{c}})=0\rightarrow T_{\text{c}}(n). \tag{22}$$

Below this temperature, the approximations (21b) describe the polar and nematic order parameters in a polar phase of a Janus fluid. This approximation is no longer applicable when the temperature $T=T_0$ with $A_2(n,T_0)=1/6$ is reached. Since the Landau–de Gennes expansion was used to derive these expressions, and the logarithm in f_{or} was expanded for weak alignment, the approximations for the order parameters can be valid only in the vicinity of the transition temperature, where the alignment is small. From their definition, the order parameters are limited to values smaller than 1. Their diverging is due to the approximations in the Landau–de Gennes expansion for f_{align}. In determining their equilibrium values (21b) from the minima of f_{align} they had the role of mere parameters in the alignment free energy.

IV. ANALYTIC RESULTS

Although it is possible to to evaluate the stated expressions for the pressure, the order parameters, and the transition temperature numerically, it is desirable to introduce another approximation which suffices to work out the influence of the anisotropy parameters $\varepsilon_{1,2,3}$ analytically. The anisotropic part ϕ^{aniso} of the full potential containing these parameters appears in the definitions for the coefficients $A_{1,2}$ and the virial coefficient $B_{2,0}^{\text{aniso}}$ through exponential functions. Let us expand the exponential function up to second order (high temperature approximation):

$$e^{-\beta\phi^{\text{aniso}}}\approx 1-\beta\phi^{\text{aniso}}+\frac{1}{2}(\beta\phi^{\text{aniso}})^2+O(|\beta\phi^{\text{aniso}}|^3). \tag{23}$$

Requiring that $|\beta\phi^{\text{aniso}}|\lesssim 1$ holds in the range of the equilibrium distance $r_{\text{eq}}^*=9/8$, where the equilibrium pair correlation function has a maximum leads to the condition $|\beta\psi|\lesssim 0.25$. In order to use the expansion (23), the anisotropy of the potential must be moderate. Considering, e.g., the ee configuration, the anisotropy parameters $\varepsilon_{1,2}$ have to satisfy $\varepsilon_{1,2}\lesssim 0.03$.

A. Coefficients $A_{1,2}$ and transition temperature T_c

Inserting Eq. (23) into the expressions (13), (17) and performing the orientational averages yields the following expressions for $A_{1,2}$:

$$A_1(n,T)=1-nI_1(T)\frac{\varepsilon_1}{T}+nI_2(T)\left(\frac{\varepsilon_3}{T}\right)^2, \tag{24}$$

$$A_2(n,T)=1-\frac{1}{5}nI_2(T)\left(\frac{\varepsilon_s}{T}\right)^2, \tag{25}$$

where $\varepsilon_s^2\equiv 3\varepsilon_1^2+5\varepsilon_2^2-\sqrt{273/10}\varepsilon_1\varepsilon_2$, and the dimensionless volumes $I_{1,2}^*=I_{1,2}r_0^{-3}$ are introduced as follows:

$$I_1^*(T)\equiv\frac{1024}{27}\pi\int_0^{3/2}(3-2r^*)^3e^{-\beta\phi^{\text{SHRAT}}(r)}(r^*)^2dr^*, \tag{26}$$

$$I_2^*(T)\equiv\left(\frac{512}{27}\right)^2\pi\int_0^{3/2}(3-2r^*)^6e^{-\beta\phi^{\text{SHRAT}}(r)}(r^*)^2dr^*. \tag{27}$$

These volumes can be viewed as averages of the first and second powers of the negative part of the spherical SHRAT potential. They are always positive and depend rather weakly on the temperature.

The temperature dependence of the coefficients $A_{1,2}(n,T)$ is shown in Fig. 4 for the dimensionless density $n^*=0.8$ and for two different sets of anisotropy parameters ε_1 and ε_2 with $\varepsilon_3=0$ representing ee and nn Janus spheres, respectively (cf. Fig. 2). For the ee Janus spheres in the diagram on top, A_1 goes through zero at the temperature $T\approx 0.8\approx T_{\text{c}}$. This is the transition temperature into the polar phase. At the temperature $T_0\approx 0.5$, $A_2=1/6$. At this temperature, the uniaxial approximation (18) for the order parameters fails, i.e., a polar phase can be expected in the temperature range $T_0\approx 0.5<T<0.8\approx T_{\text{c}}$.

For the nn Janus spheres of the right-hand diagram of Fig. 4, we see that $T_0>T_{\text{c}}$. Therefore a polar phase is not expected and it is worth examining this parameter region via Monte Carlo simulation.

The form (24) reveals that A_1 can only have a zero, and a polar phase is predicted [cf. Eq. (22)], for $\varepsilon_1>0$ (since $I_{1,2}>0$). As Fig. 4 reveals, this is even further restricted to systems of ee Janus spheres. Furthermore, expressions (22), (24) show that a nonvanishing ε_3 reduces T_c, while T_c is insensitive to the value of ε_2. But A_2 does depend on ε_2 and therefore ε_2 has an effect on T_0. Therefore, the choice of ε_2 in relation to ε_1 is essential for the presence of a uniaxial polar phase and its range of existence in parameter space.

B. Alignment free energy

With the high temperature expansion (24), upon inserting $A_{1,2}$ from Eqs. (24),(25) into the free energy $f_{\text{align}}^{\text{LdG}}(n,T)$ associated with the alignment (19), we obtain

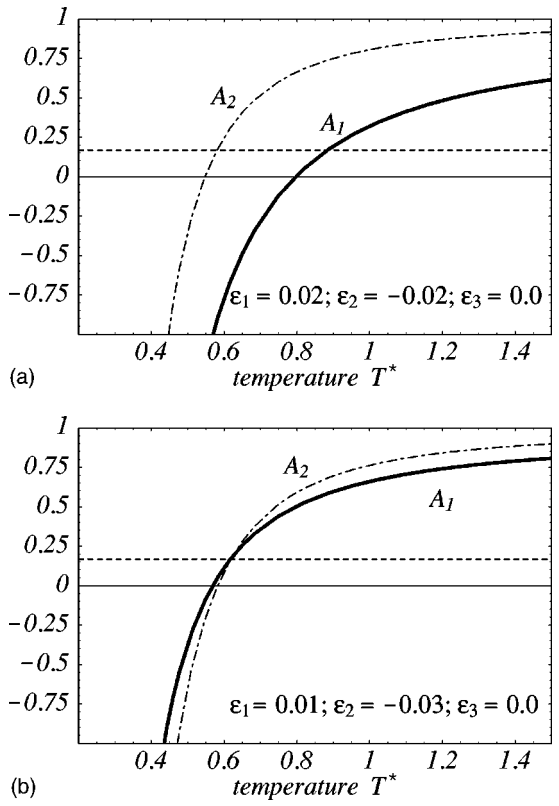

FIG. 4. The coefficients $A_1(n,T)$ and $A_2(n,T)$ at a density $n^*=0.8$ and anisotropy parameters $\varepsilon_3=0.0$ and $(\varepsilon_1;\varepsilon_2)=(0.02;-0.02)$ (top) $[(0.01;-0.03)$ (bottom)]; the dashed horizontal curve is at a value of 1/6. The zero of $A_1(n,T)$ marks the transition temperature T_c, the intersection of $A_2(n,T)$ with the dash-dotted curve marks that temperature where the order parameters (21b) diverge (see Sec. III E). The dimensionless temperature is denoted as T^* in the figure. For convenience, T and T^* are used synonymously in the text part.

$$f_{\text{align}}^{\text{LdG}}=\frac{k_BT}{2}\left[1-nI_1(T)\frac{\varepsilon_1}{T}+nI_2(T)\left(\frac{\varepsilon_3}{T}\right)^2-2S_2\right]3S_1^2+\frac{k_BT}{2}\left\{\frac{54}{5}S_1^4+\left[5-nI_2(T)\left(\frac{\varepsilon_s}{T}\right)^2\right]S_2^2\right\}. \quad (28)$$

Figure 5 shows a plot of the alignment free energy as a function of the order parameters $S_{1,2}$ for the reduced density $n^*=0.8$ and the anisotropy parameters $\varepsilon_1=-\varepsilon_2=0.02$ and $\varepsilon_3=0$ (ee Janus spheres) at temperature $T=0.87$. At this temperature there is a single minimum for vanishing order parameters. The alignment free energy f_{align} is symmetric in S_1 but asymmetric with respect to S_2. The positive value for the nematic order parameter shows that the particle axes are mostly aligned along the director axis rather than perpendicular to it. For the temperature $T=0.72$ below the transition temperature $T_c\approx 0.8$ into a polar phase, there are two minima for positive (and unphysical negative, thus irrelevant) values of the polar order parameter S_1 and a positive nematic order parameter S_2.

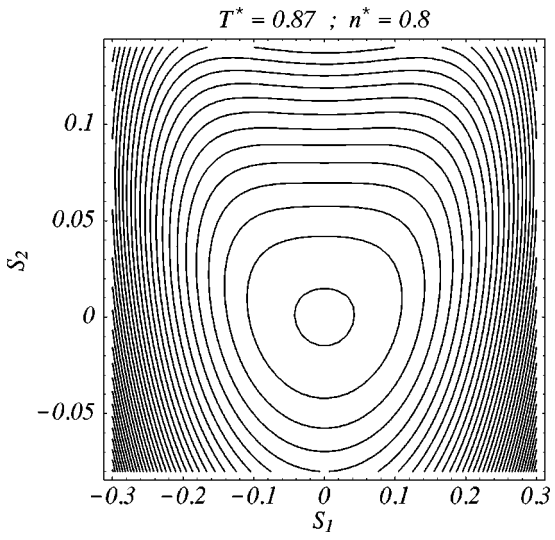

FIG. 5. The alignment free energy f_{align} from Eq. (28) as a function of the order parameters $S_{1,2}$. The density is $n^*=0.8$, the anisotropy parameters are $\varepsilon_1=0.02$, $\varepsilon_2=-0.02$, and $\varepsilon_3=0.0$. The temperature is $T=0.87$, which is above the transition temperature (cf. Fig. 4). The single minimum of the free energy is located in the center of the diagram; contour lines are drawn in equidistant energy steps. The expected symmetry of f_{align} with respect to S_1 and asymmetry with respect to S_2 can be seen clearly. The minimum of f_{align} at vanishing order parameters disappears below the transition temperature and two minima occur (not plotted) with nonvanishing order parameters.

C. Order parameters

The positions of the minima of f_{align} are given by the expressions (21b) for the order parameters in terms of the explicit expressions for the coefficients $A_{1,2}$ [Eqs. (24),(25)]. As shown above in Sec. IV A, a nonzero order parameter S_1 is expected only for ee Janus spheres with $\varepsilon_1>0$; we mostly consider ee spheres in the remainder of this section. The order parameters are shown in Fig. 6 as function of the temperature ($n^*=0.8$). The anisotropy parameters are $\varepsilon_1=-\varepsilon_2=0.02$ and $\varepsilon_3=0$ (thinnest curve). For temperatures just

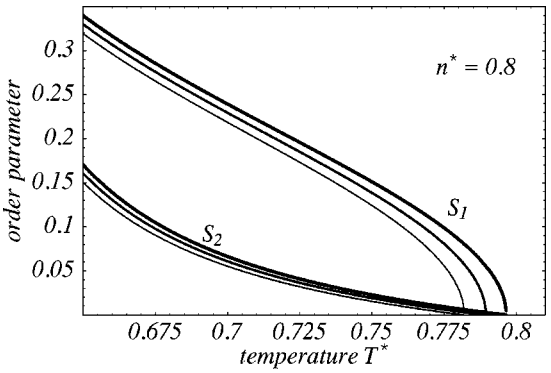

FIG. 6. Influence of temperature and ε_3 on the polar and nematic order parameters S_1 and S_2 at $n^*=0.8$, $\varepsilon_1=0.02$, $\varepsilon_2=-0.02$, and $\varepsilon_3=0,0.007,0.01$ (thinning curves). By varying the density (results not shown) we find that the transition temperature T_c is slightly increasing with increasing density.

below the transition temperature T_c, the polar order parameter grows rapidly. At lower temperatures the increase is almost linear. The nematic order parameter S_2 remains much smaller than the polar order parameter S_1. For very low temperatures the increase of the order parameters is stronger again. This is where the second coefficient A_2 approaches 1/6 and the expression for the order parameter diverges. By varying the density (results not shown) we find that the transition temperature T_c is slightly increasing with increasing density; see Sec. IV E and Fig. 9 for further discussion. Figure 6 also shows the influence of the third anisotropy parameter ε_3 on the order parameters. The transition temperature and the order parameters decrease with increasing absolute value for ε_3 [which appears quadratic in expression Eq. (24)].

D. Pressure of a Janus fluid in its isotropic and polar phases

Applying the high temperature approximation (23) to expression (11) for the virial coefficient $B_{2,0}^{\mathrm{aniso}}$ yields

$$B_{2,0}^{\mathrm{aniso}}(T) = -(3\varepsilon_1^2 + 5\varepsilon_2^2 + 9\varepsilon_3^2)(2T)^{-2} I_2(T). \qquad (29)$$

This expression is always negative and the contribution $p_{\mathrm{iso}}^{\mathrm{aniso}}(n,T) = n^2 k_{\mathrm{B}} T B_{2,0}^{\mathrm{aniso}}(T)$ originated by the anisotropic part ϕ^{aniso} of the model potential to the pressure p_{iso} in the isotropic phase of the fluid is also negative. The pressure of the isotropic Janus fluid with its nonspherical interaction is smaller than that of a SHRAT fluid with purely spherical interaction. The anisotropy enters into Eq. (11) through the sum $(3\varepsilon_1^2 + 5\varepsilon_2^2 + 9\varepsilon_3^2)$ of squares of the anisotropy parameters. Thus, the pressure depends only on the strength of anisotropy of the potential, but not on the signs of the anisotropy parameters. Due to this reduction of the pressure, an isotropic Janus fluid will also have a critical temperature which is below the one for a SHRAT fluid.

The different contributions to the pressure of a Janus fluid in its isotropic phase—p_{kin}, p_{rep}, $p_{\mathrm{dis}}^{\mathrm{iso}}$, and $p_{\mathrm{iso}}^{\mathrm{aniso}}$, respectively, with the high temperature approximation (29) applied for the last expression—are displayed graphically in Fig. 7. The temperature chosen was $T = 0.6$ and the anisotropy parameters for the ee Janus spheres are $\varepsilon_1 = -\varepsilon_2 = 0.02$ and $\varepsilon_3 = 0$. The linear kinetic and the Carnahan-Starling term give positive contributions, whereas the virial expressions, quadratic in the density, are negative. The Carnahan-Starling part is displayed separately, because it grows rapidly for larger densities.

The alignment pressure p_{align} is displayed in Fig. 7 (inset). In Eq. (20) for p_{align} the expressions (18) are inserted for the order parameters and the high temperature approximation (24),(25) is used for $A_{1,2}(n,T)$. The pressure is is zero for densities below the ''transition density'' n_c. Here, $n_c^* \approx 0.5$ for this given temperature. Above this density it is negative and very small, so that the difference between the pressures in the isotropic and the polar phase should be very small. For higher densities p_{align} diverges, while the Landau–de Gennes energy approximation in terms of order parameters becomes invalid.

The total pressure of the Janus fluid, i.e., the sum of all the contributions from Fig. 7, is displayed in Fig. 8 for two selected temperatures as function of the density. Anisotropy parameters are chosen as before. For low densities in the gaseous phase, the increase of the pressure is almost linear due to the kinetic contribution. Below the critical temperature T_c, the derivative of the pressure with respect to n is negative for intermediate densities, i.e., in the region of coexistence between gas and liquid phases. For high densities as the repulsion between the particles becomes important, the Carnahan-Starling term starts dominating and the pressure increases. The lower diagram in Fig. 8 shows the pressure at a temperature close to the critical temperature of the Janus fluid and the SHRAT fluid. For the latter it is slightly higher due to the influence of the anisotropic part of the potential in the Janus fluid. However, the value of the shift is not very reliable, because a mean field theory like the virial expansion cannot correctly describe the critical behavior of a fluid that is governed by fluctuations.

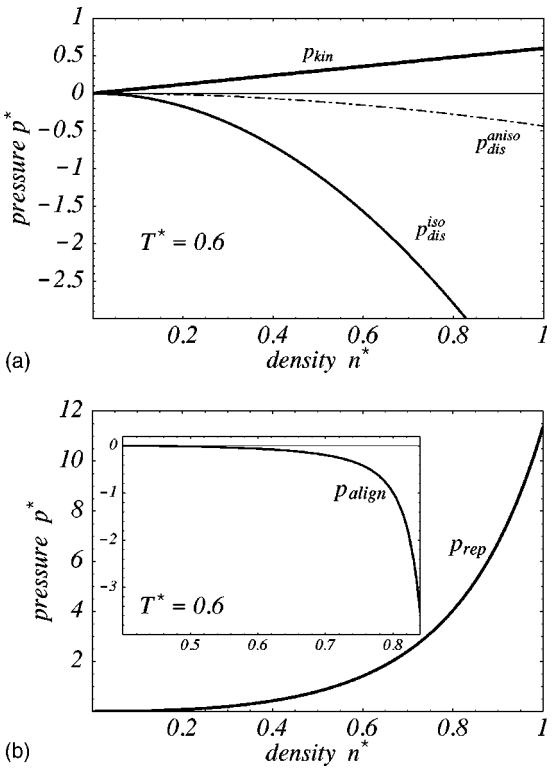

FIG. 7. The contributions p_{kin}, $p_{\mathrm{dis}}^{\mathrm{iso}}$, and $p_{\mathrm{dis}}^{\mathrm{aniso}}$ (top) and p_{rep} (bottom) as well as the alignment contribution $p_{\mathrm{align}}(n,T) = p_{\mathrm{dis}}^{\mathrm{align}}(n,T)$ (bottom inset) to the pressure of an isotropic Janus fluid with $\varepsilon_1 = 0.02$, $\varepsilon_2 = -0.02$, and $\varepsilon_3 = 0$ as a function of density at a temperature of $T = 0.6$. For $p_{\mathrm{dis}}^{\mathrm{aniso}}$ the high temperature approximation (29) was applied.

E. Qualitative phase diagram

Using the above results for the pressure and evaluating conditions for the stability of different phases, we can construct a qualitative phase diagram of the Janus fluid made of ee spheres in the (n,T) plane. Such a phase diagram for a special choice of anisotropy parameters is depicted in Fig. 9. The diagram shows the regions of liquid and gaseous single

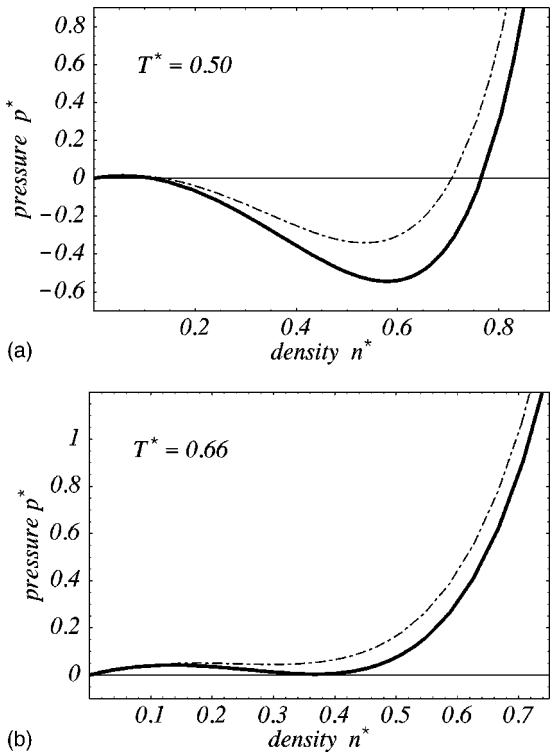

FIG. 8. The total pressure of a SHRAT fluid (dash-dotted curve) and an isotropic Janus fluid with $\varepsilon_1=-\varepsilon_2=0.02$ and $\varepsilon_3=0$ (solid curve) as a function of the particle density at two selected temperatures. The lower diagram shows the pressure at a temperature close to the critical temperature $T_{\mathrm{crit}}=0.66$ of the SHRAT fluid and $T_{\mathrm{crit}}=0.71$ of the Janus fluid. For $p_{\mathrm{dis}}^{\mathrm{aniso}}$ the high temperature approximation (11) was applied.

phase and the two-phase region of coexisting liquid and gaseous phases. The fluid phase is marked for temperatures above the critical temperature T_{crit} of the Janus fluid. The two-phase region is approximately determined by the spinodal curve $T_{\mathrm{sp}}(n)$, which connects the extrema with respect to the density n of the pressure curve $p(n,T)$ and is derived from the condition $(\partial p/\partial n)[n,T_{\mathrm{sp}}(n)]=0$. The vertex of the spinodal at the critical density/critical temperature pair $(n^*_{\mathrm{crit}},T_{\mathrm{crit}})\approx(0.23,0.71)$ marks the critical point of the fluid. Above the critical temperature T_{crit} is the fluid phase without distinction between liquid and gaseous phases. In an absolutely stable phase of a fluid, not only the derivative, but the pressure itself must be positive. For higher densities above $n^*\approx 0.35$, the corresponding condition $p[n,T(n)]=0$ yields an approximation for the bounds of the two-phase region which improves upon the approximation based on the spinodal.

Isotropic and polar liquid phases are separated by the curve $T_c(n)$ with $T_c=nI(T_c)\varepsilon_1$. This equation follows from condition (22), $A_1[n,T_c(n)]=0$, with A_1 from Eq. (24), when $\varepsilon_3=0$ (which is the case for the phase diagram shown in Fig. 9). Since $I_1(T)$ is weakly dependent on the temperature in the vicinity of $T=0.8$ we estimated the critical temperature shown in Fig. 9 from the condition $T_c(n)=nI_1(T=0.8\phi_0/k_B)\varepsilon_1$, where $\varepsilon_1=0.02$.

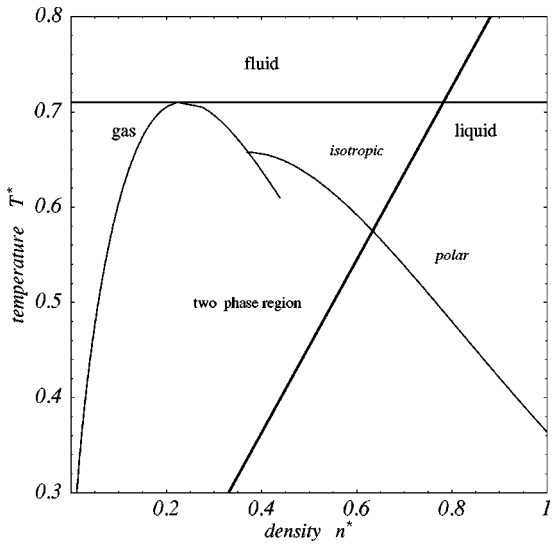

FIG. 9. Phase diagram for a Janus fluid with anisotropy parameters $\varepsilon_1=-\varepsilon_2=0.02$ and $\varepsilon_3=0$. Below the density $n^*=0.35$ the extension of the two-phase region is determined from the spinodal T_{sp}; above this density from the zero $p(n,T)=0$ of the pressure. The kink in the thin bent curve results from these conditions. The horizontal straight line marks the critical temperature T_{crit} and separates the fluid from the gaseous and liquid phases. The thick straight line increasing linearly with density is the transition temperature $T_{\mathrm{c}}(n)$ from isotropic to polar liquid according to Sec. IV E.

F. Range of validity and possible correction

For low temperatures, the equation of state (14) describes the numerical results to be discussed in the next section only for very low densities in the gaseous phase and for high densities in the liquid phase. At intermediate densities in the region of coexistence of gas and liquid the pressure is not described correctly. In Ref. [22] the pressure of a spherical SHRAT fluid was calculated analytically employing an augmented van der Waals approximation as well as numerically via molecular dynamics (MD) simulation. Compared with the MD results, the augmented van der Waals approximation yielded a too high pressure. Applying a temperature and density dependent ''correction term'' $c(n,T)$ to the distortion pressure p_{dis}, i.e., replacing p_{dis} by $p_{\mathrm{dis}}[1+c(n,T)]$ in the equation of state, with a particular simple correction the simulation results are well described. The correction term, motivated by increased fluctuations in the two-phase region, keeps the limiting correct behaviors, $c(0,T)=0$, $c(n,0+)=0$, and a dimensionless density appears as a product between n and the effective volume introduced above. The correction term employed first used in [22], reads $c(n,T)=[3nv_{\mathrm{eff}}(T)+6n^2v_{\mathrm{eff}}^2(T)]e^{-\beta\phi_0}$. Simulation results to be presented next will be compared with both the uncorrected and the corrected expressions discussed in this section.

V. NUMERICAL RESULTS

A. *NVT* Monte Carlo simulation setup

In the following, we report results of Monte Carlo (MC) simulations for configurational properties of the same model for Janus fluids without referring to any approximation apart

from possible finite size effects. The MC simulations were carried out in an *NVT* or canonical ensemble with constant number of particles *N*, constant volume *V*, and temperature *T*. The particles (Janus spheres) of the Janus fluid were enclosed in a cubic central simulation box with volume *V*. Periodic boundary conditions were applied to reduce the effects of finite system size, and the minimum image convention was used [23]. A Janus sphere is described by the spatial coordinates of the center of mass and the direction of the unit axis vector $\mathbf{u}$. If it is attempted to move a particle in the simulation, with equal probability the center of mass is shifted in space or the axis vector is rotated around one of the three spatial coordinate axes. The axis of rotation is chosen with probability 1/3, and we used the Metropolis algorithm [24], i.e., an attempted move of a particle is accepted with the probability $W_{\mu\nu} \propto \min(1, \exp\{-\beta \Delta E_{\mu\nu}^{\mathrm{pot}}\})$, where $\Delta E_{\mu\nu}^{\mathrm{pot}} = E_{\nu}^{\mathrm{pot}} - E_{\mu}^{\mathrm{pot}}$ is the difference of potential energy of the new configuration E_{ν}^{pot} (after the particle was moved) and the previous configuration E_{μ}^{pot} (before the particle was moved). A full Monte Carlo step includes an attempted move of all particles of the fluid. Our systems relaxed for several thousand MC steps, before averages of configurational properties were extracted during several thousand further MC steps. The configurations after every tenth MC step are used for the sample set to calculate the MC averages. This was done to reduce correlations between subsequent configurations and improve the accuracy of the averages [25]. Averages are accumulated as mean values over MC realizations as follows.

The potential part of the symmetric part of the pressure tensor $\mathbf{p}_{\mathrm{pot}}$ is calculated with the virial expression $\mathbf{p}_{\mathrm{pot}} V = \langle \Sigma_{i=1}^{N} \Sigma_{j=i+1}^{N} \mathbf{r}_{ij} \mathbf{F}(\mathbf{r}_{ij}, \mathbf{u}_i, \mathbf{u}_j) \rangle$, where $\mathbf{F} = -\nabla_{\mathbf{r}_{ij}} \phi$ is the force acting between two Janus spheres, resulting from the gradient of the binary interaction potential ϕ, and $\mathbf{r}_{ij} = \mathbf{r}_i - \mathbf{r}_j$ is the distance vector of two particles. To receive the full symmetric pressure tensor, the kinetic (isotropic) pressure $\mathbf{p}_{\mathrm{kin}} = n k_{\mathrm{B}} T \mathbf{1}$ is added: $\mathbf{p} = \mathbf{p}_{\mathrm{pot}} + \mathbf{p}_{\mathrm{kin}}$. The scalar pressure is obtained as $p = (1/3)\mathrm{Tr}\mathbf{p}$, since the existing torques do not contribute to the trace of the full pressure tensor. From the MC results, the average for the potential energy per particle u_{pot} is obtained as $u_{\mathrm{pot}} = \langle \Sigma_i' \Sigma_{j>i} \phi(\mathbf{r}_{ij}, \mathbf{u}_i, \mathbf{u}_j) \rangle$, where the symbol Σ_i' denotes the normalized sum $\Sigma_i' \equiv (1/N) \Sigma_{i=1}^{N}$ with N being the number of particles, and $\langle \cdots \rangle$ stands for the ensemble average. The polar order parameter S_1 is calculated by taking the norm of the mean axis vector $\mathbf{u} \equiv \Sigma_i' \mathbf{u}_i$, i.e., $S_1 = \langle |\mathbf{u}| \rangle$, i.e., $S_1 = 1 \ \forall_i \ \mathbf{u}_i = \mathbf{u}$, since $|\mathbf{u}_i| = 1$. Similarly, the amplitude of the order parameter S_2 is obtained from the relation

$$S_2^2 = (3/2) \langle (\Sigma_i' \overline{\mathbf{u}_i \mathbf{u}_i} : \Sigma_i' \overline{\mathbf{u}_i \mathbf{u}_i})^{1/2} \rangle$$

The sign of the nematic order parameter is obtained using the relation $S_2 \propto \langle (\mathbf{n} \cdot \Sigma_i' \mathbf{u}_i)^2 - 1/3 \rangle$, where $\Sigma' \mathbf{u}$ is the average axis vector in a single configuration.

Simulation results to be presented in the following are obtained as follows. In the pressure calculations in Secs. V B and V C, *single* simulations with a given number of particles N (typically $N = 1024$), fixed overall particle number density n, and fixed temperature T, were carried out with random start configurations (initial positions of the particles on a fcc lattice when mentioned explicitly). The duration of a simulation was usually $M = 2 \times 10^4$ MC steps. In obtaining the results of Sec. V D, for a given density n a *series* of *NVT* MC simulations was initiated with random start configurations at a relatively high temperature. The temperature was then successively reduced (if not otherwise mentioned) at a rate $\Delta T = 0.02$ per $M = 2 \times 10^4$ MC steps. At a low temperature this process was reversed and the temperature was increased again. The results for the different branches of the simulation may differ. The hysteresis effects should mainly be due to the finite rate. In the transition regimes isotropic-nematic and isotropic-polar, where the hysteresis effects are most pronounced, the duration of the simulation was increased ($M = 4 \times 10^4$).

The first 10^4 MC steps at a new temperature were always disregarded for taking averages. The anisotropy parameters are set such that the potential ϕ models amphiphilic Janus spheres; corresponding estimates were discussed above. Furthermore, in order to potentially observe a polar phase, $\varepsilon_1 > 0$ is chosen.

B. The pressure of the SHRAT and Janus fluid

Figure 10 shows MC results for the pressure of the Janus fluid (with $\varepsilon_1 = -\varepsilon_2 = 0.02$, $\varepsilon_3 = 0$) as well as for the SHRAT fluid as a function of density for different temperatures. We compare with the analytical results derived in the foregoing sections, earlier results for the SHRAT fluid obtained via molecular dynamics simulation, approximated by the corrected equation of state described in Sec. IV F. The diagrams of Fig. 10 confirm that the augmented van der Waals approximation tends to overestimate the value for the pressure. For the temperatures $T = 0.8$, 1.0, and 2.0, which are above the critical temperatures for the SHRAT and Janus fluids (not all results plotted), the corrected equation of state agrees well with the MC results for the full range of densities shown, for both types of fluids. The MC results for the SHRAT fluid are identical to the ones obtained via MD within the range of accuracy of [22]. Also, for temperatures below the critical temperature, e.g., $T = 0.5$, the corrected equation of state generally describes the pressure of the fluid correctly in the single phase regions with very high and very low densities. Only the fluctuation dominated behavior of the two-phase region cannot be described with a mean field theory such as the one employed here. In these regions, the local particle density becomes inhomogeneous. ''Holes,'' regions with very low density, are formed, as can be seen in the snapshot of the fluid shown in Fig. 11. Therefore, the MC results are not accurate in the two-phase region, because the virial expression for the pressure requires a homogeneous system.

C. The liquid phase of the Janus fluid

The realm of the liquid phase of a fluid composed of particles with a very short range of interaction can be very narrow; for a fluid of C_{60} fullerenes, Hagen *et. al.* in [26] suppose that there exists no liquid phase at all. As an indica-

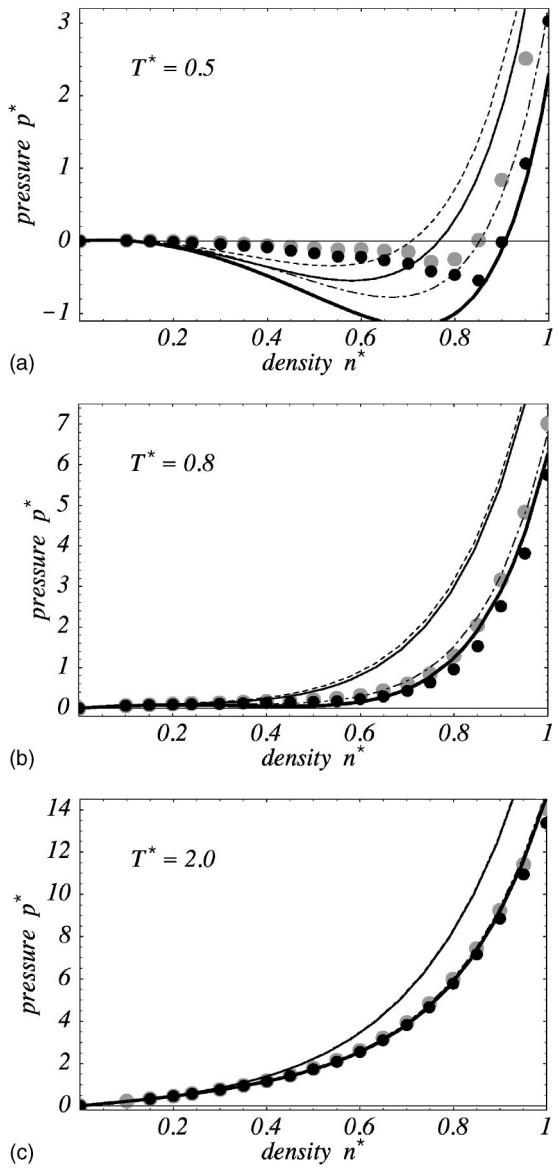

FIG. 10. The pressure as a function of the density: the dashed and the dash-dotted curves represent the augmented van der Waals approximation from Eq. (14) and the corrected equation of state (cf. Sec. IV F), respectively, for the SHRAT fluid. The thin and thick solid lines give the according expressions for a Janus fluid with anisotropy parameters $\varepsilon_1 = -\varepsilon_2 = 0.02$ and $\varepsilon_3 = 0$. For the contribution $p_{\mathrm{dis}}^{\mathrm{aniso}}$ in the equations of state of the Janus fluid the high temperature approximation (11) was applied. The gray dots are the results of the MC simulations in the SHRAT fluid; the black dots are those for the Janus fluid. The number of particles used in the simulation was $N = 1024$. In a simulation, the start configuration was chosen randomly, the system was relaxed for 10^4 MC steps, and averages were extracted over 10^4 MC steps.

tion of where the liquid phase and therefore anisotropic, liquid crystalline phases of a Janus fluid could be found, the pressure in systems of Janus spheres with unordered initial configuration was compared to the pressure of a system with fcc crystalline initial configuration. The results are displayed in Fig. 12 for two different temperatures.

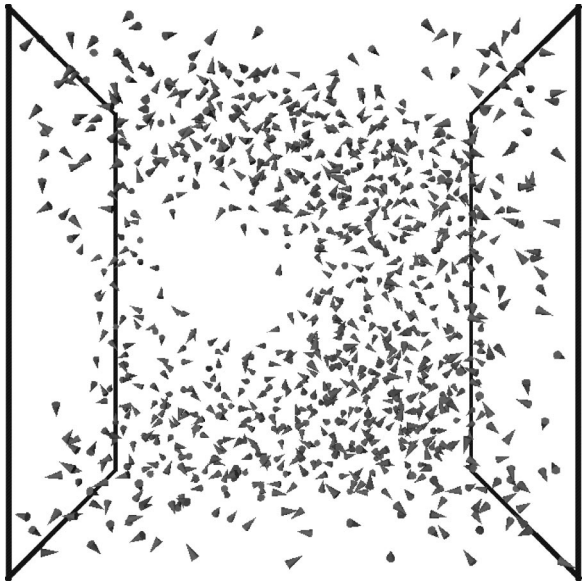

FIG. 11. The perspective view of this snapshot from the Janus fluid in the two-phase region at $T = 0.5$ and $n^* = 0.5$ shows the formation of areas with high and low densities in the fluid. The Janus spheres are represented as cones; the frames mark the edges of the central simulation box.

Along with the numerical results, Fig. 12 shows the analytic results for the pressure of the isotropic fluid according to the augmented van der Waals equation of state (14) and the corrected equation of state (cf. Sec. IV F), again with the high temperature expansion applied to $p_{\mathrm{iso}}^{\mathrm{aniso}}$. Comparison of the corrected equation of state and the MC results for the pressure of the unordered, fluid system reveals good agreement outside the two-phase region. For high densities a weak alignment of the particles' axes, with $S_1 \lesssim 0.3$, is observed in the MC simulations. Since the alignment part p_{align} of the pressure is not considered for correction in Sec. IV F, the good agreement between the pressure curves confirms the finding of Sec. IV D that the alignment pressure is negligible for small order parameters.

For given density, the pressure in the crystalline system is smaller—and the increase of the pressure with the density is larger—than in the unordered, fluid system. The pressure in the fcc phase becomes negative for densities below $n^* \approx 0.95$ and this phase cannot be absolutely stable for smaller values. For $n^* \approx 0.85$, the pressure reaches the value obtained for the fluid system. At this density, the crystalline order disappears and a transition to the fluid phase occurs. The pressure in the fluid phase is positive above $n^* \approx 0.8$ and thus, a liquid phase of the system might be located in the density range of $0.8 \lesssim n^* \lesssim 0.9$.

D. Anisotropic phases in Janus fluids

Via Monte Carlo simulations, anisotropic phases with polar and nematiclike order are found with different sets of order parameters.

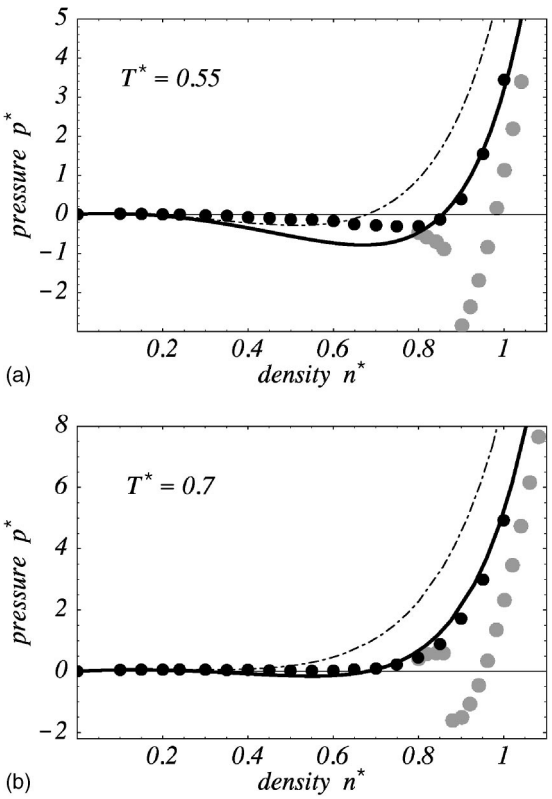

FIG. 12. The pressure of a fluid and a fcc crystal of Janus spheres with anisotropy parameters $\varepsilon_1 = -\varepsilon_2 = 0.02$ and $\varepsilon_3 = 0$ for two selected temperatures; the black dots give the results of an unordered start configuration, the gray dots those with fcc start configuration. The dash-dotted curves represent the pressure of the fluid, calculated with the equation of state [cf. Eq. (14)]. The solid line is the pressure according to the corrected equation of state (cf. Sec. IV F). The number of particles in the simulations with the unordered start configuration was $N = 1024$; in the fcc start configuration it was $N = 864$. The system was relaxed for 10^4 MC steps and averages were extracted over 10^4 MC steps in both cases.

1. Polar phases for ee Janus spheres

A polar alignment of the particle axes, as predicted in Secs. III and IV, is found from our MC simulation for the case of ee Janus spheres.

(a) Janus fluid with $\varepsilon_1 = -\varepsilon_2 = 0.03$, $\varepsilon_3 = 0$. Results for the order parameters, the pressure, and the potential energy of the particular Janus fluid are displayed as functions of the density in Fig. 13. The upper left diagram in this figure shows the behavior of the order parameters $S_{1,2}$ vs temperature. Above the transition temperature $T_c \approx 0.62$, the order parameters are small, with $S_{1,2} \lesssim 0.1$. Below the transition temperature the polar order parameter increases rapidly up to a value of $S_1 \approx 0.6$ at $T = 0.56$, and then continues increasing with decreasing temperature up to a value of $S_1 \approx 0.8$ at $T = 0.3$, which describes an almost total alignment of the particles. The nematic order parameter S_2 is much smaller than S_1. The system is in a polar phase. The alignment of the particles is shown in the snapshot from the fluid in Fig. 14. This snapshot also reveals the existence of a hole in the fluid. The contraction of the fluid that leaves regions with very low density is also reflected in the pressure diagram in the middle

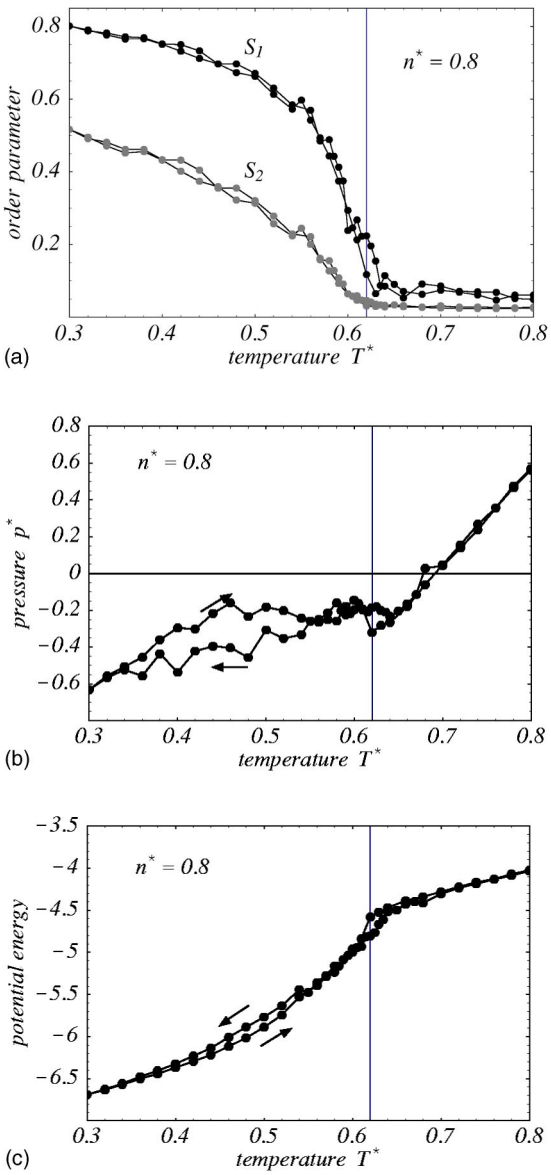

FIG. 13. Order parameters S_1 and S_2, the pressure and the potential energy per particle of in system of Janus spheres with anisotropy parameters $\varepsilon_1 = -\varepsilon_2 = 0.03$ and $\varepsilon_3 = 0$ as functions of temperature. The number of Janus spheres is $N = 2048$ and the average density is $n^* = 0.8$. The vertical line marks the transition temperature; the arrows indicate the heating/cooling branches.

of Fig. 13. For higher densities, the pressure falls almost linearly with decreasing temperature, and vice versa. The pressure is negative for temperatures below $T \approx 0.7$. That means that the polar phase in the fluid can only be metastable. For $T \lesssim 0.62$ the pressure remains constant (apart from some fluctuations) while reducing temperature. It is this range where the fluid contracts and inhomogeneities appear. This contraction is finished at $T \approx 0.34$ where the pressure starts decreasing with the temperature again. The temperature $T = 0.62$ equals the transition temperature. This coincidence may be accidental, although a contraction of the fluid might enforce the alignment of the particles, or vice versa, an alignment of the particles might induce the contraction, be-

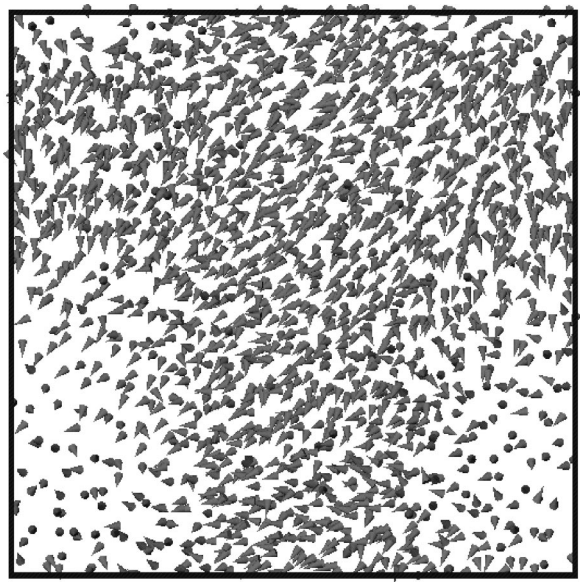

FIG. 14. The snapshot from the polar phase of a Janus fluid with anisotropy parameters $\varepsilon_1 = -\varepsilon_2 = 0.03$ and $\varepsilon_3 = 0$ consisting of $N = 2048$ particles at an average density of $n^* = 0.8$ shows the orientational order of the system with a preferred direction of the particle axes pointing from the upper right to the lower left.

cause the average equilibrium distance between two particles is reduced. The contraction of the fluid and the reduction of the average distance between the particles is also reflected in the behavior of the potential energy. Its decrease is stronger in the range of the contraction with approximately constant pressure than in the other regions. For the quantities pressure and potential energy a hysteresis between heating/cooling branches of the MC run (with $M = 4 \times 10^4$) is present only for low temperatures, while we do not detect any hysteresis for the order parameters.

(b) Janus fluid with $\varepsilon_1 = 0.02$, $\varepsilon_2 = -0.02$, $\varepsilon_3 = 0$. Figure 15 shows results of MC simulations for order parameters, pressure, and potential energy per particle of a Janus fluid with the anisotropy parameters $\varepsilon_1 = -\varepsilon_2 = 0.02$, $\varepsilon_3 = 0.0$. The results are quite similar to those in Fig. 13. The transition temperature from the isotropic to the polar phase is $T \approx 0.49$ is smaller than before. The order parameters are smaller as well, with a maximum value of $S_1 \approx 0.7$ for the polar order parameter at $T = 0.3$. The values for the anisotropy parameters have been used to display analytical results in Sec. IV (cf. Fig. 6). Compared with those, the transition temperature is considerably smaller here ($T_c \approx 0.49$ for the MC results compared to $T_c \approx 0.8$ for the analytic results). The order parameters calculated in the simulations on the other hand are much larger compared with their analytically calculated counterparts. In the transition region were the approximate expressions (21b) hold, the calculations give $S_1 \lesssim 0.2$, whereas the simulations give values of $S_1 \lesssim 0.5$ for the polar order parameter.

The number of particles N, the average density n^*, and the duration of the simulations were chosen as before. In the range of the transition into the polar phase, again simulations with longer duration were carried out to improve the accuracy. This was done in the cooled as well as in the heated branch. The hysteresis, however, did not disappear as was the case before. Especially for the potential energy per particle there is a large difference between the two branches, with the energy being almost constant when the temperature is increased from $T = 0.46$ to $T = 0.52$. In this range the system starts to crystallize, before it becomes fluid again at $T = 0.54$, where the values for the energy reach those of the cooled fluid. The solidification begins at increasing temperature. This indicates that he relaxation time allowed to the fluid was not sufficient. This is confirmed by selected simulations with relaxation times of 4×10^5 MC steps at temperatures of $T = 0.44$, 0.56, and 0.58 shown in the diagrams. The

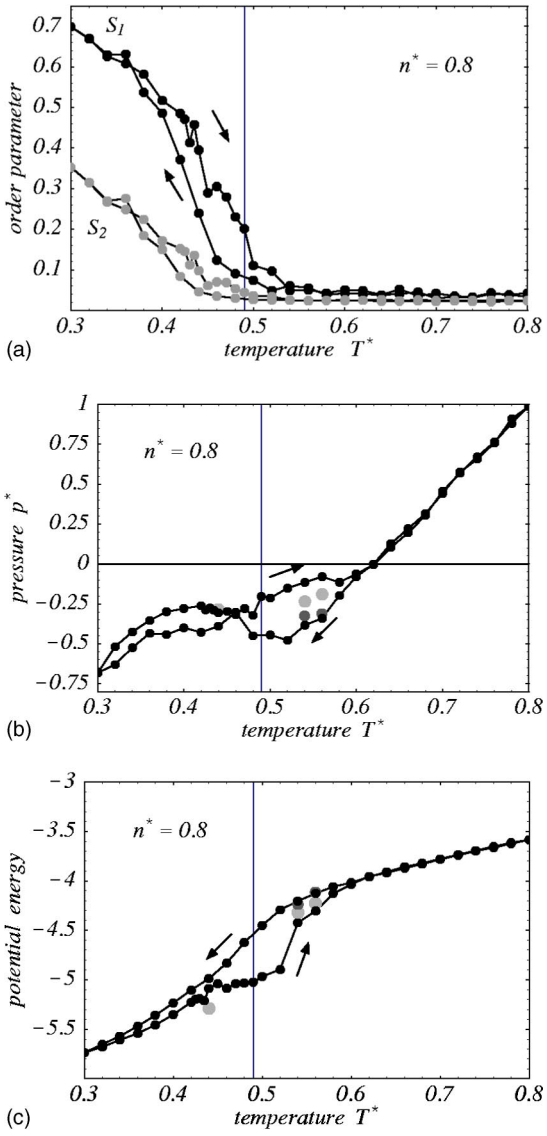

FIG. 15. Order parameters S_1 and S_2, the pressure, and the potential energy per particle of a system of Janus spheres with anisotropy parameters $\varepsilon_1 = -\varepsilon_2 = 0.02$ and $\varepsilon_3 = 0$ as function of temperature. The number of Janus particles is $N = 2048$ and the average density is $n^* = 0.8$. The vertical line marks the transition temperature; the arrows indicate the heating/cooling branch. The single gray dots in the pressure and potential energy diagrams show results of simulations with enlarged duration of the simulation.

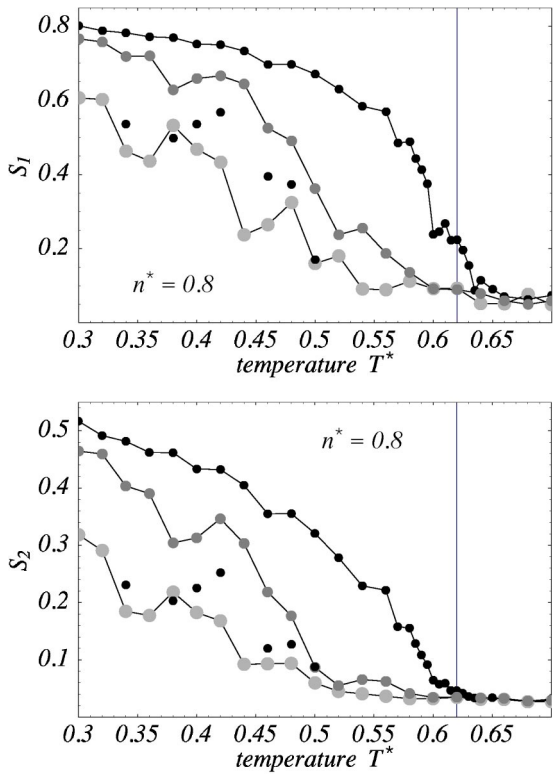

FIG. 16. Influence of ε_3 on the polar and nematic order parameter S_1 (top) and S_2 (bottom). The anisotropy parameters are $\varepsilon_1 = -\varepsilon_2 = 0.03$, $\varepsilon_3 = 0$ (black dots), $\varepsilon_3 = 0.01$ (dark gray dots), and $\varepsilon_3 = 0.014$ (light gray dots).The particle number in the simulation was $N = 2048$ and the average density is $n^* = 0.8$. The relaxation time in the additional simulations with nonzero ε_3 was 5×10^4 MC steps and the averages were extracted over 2×10^4. The single black dots represent results for $\varepsilon_3 = -0.014$.

polar phase for this Janus fluid is not liquid anymore and should be glasslike. In the simulation described in the paragraph before, no signs of crystallization were observed, even for a simulation with 5×10^5 MC steps at $T = 0.54$. For that particular Janus fluid, a liquid polar phase might exist, at least in the transition region near T_c.

(c) Influence of ε_3. The discussions in Sec. IV have shown that a nonvanishing third anisotropy parameter ε_3 reduces the amount of order in the Janus fluid and also reduces the transition temperature into a polar phase. This result was qualitatively confirmed with MC simulations for which results are displayed in Fig. 16 for a Janus fluid with basic anisotropy parameters $\varepsilon_1 = -\varepsilon_2 = 0.03$, and the three different values $\varepsilon_3 = 0, 0.01, 0.014$. The ratio of ε_3 to $\varepsilon_{1,2}$ is therefore comparable to that in Fig. 6. For $\varepsilon_3 = 0$ the results from Fig. 13 were used; the final configurations of these simulations served as new initial configurations with $\varepsilon_3 = 0.01$ and these final configurations were then used for the simulations with $\varepsilon_3 = 0.014$. The results show that the order parameters S_1 and S_2 are reduced through the influence of ε_3, although the effect seems to be stronger than analytically forecast. At some selected temperatures, simulations with negative $\varepsilon_3 = -0.014$ were carried out. The results are qualitatively equal to those with positive ε_3. The sign of ε_3 does not seem to matter as predicted in Sec. IV.

2. Pseudonematic phases in nn Janus fluids

The discussions of the analytic results in Sec. IV have revealed that for certain sets of anisotropy parameters representing proper (nn) Janus spheres with positive values for ε_1, no polar phase can be described with the analytic expressions (21b) for the order parameters (cf. Fig. 4). Results of MC simulation in a Janus fluid with anisotropy parameters $\varepsilon_1 = 0.01$, $\varepsilon_2 = -0.03$, $\varepsilon_3 = 0$ are displayed in Fig. 17. They show that the system can enter an anisotropic phase with a nematiclike order characterized by a vanishing polar order parameter S_1 and nonvanishing nematic order parameter S_2. This phase will be referred to as a pseudonematic phase.

The upperleft diagram in Fig. 17 shows that the polar order parameter S_1 vanishes for all temperatures. In the cooled branch of the simulation, the nematic order parameter S_2 starts to increase below the temperature $T = 0.4$ up to a value of $S_2 = 0.7$ at $T = 0.3$. Simultaneously a strong positional order in the fluid is induced and the system crystallizes. The particles form planes with a common preferred direction of the particle axes, which is reversed in the neighboring plane, and thus exhibit a smectic A_d phase (experimentally observed in mixtures of polar compounds). As the system is reheated, S_2 is reduced slowly; the alignment of the particles is finally resolved at the temperature $T = 0.68$. The behavior of the pressure of the cooled fluid is similar to that observed in the previous simulations. It is negative below $T \approx 0.66$ and is hardly reduced with reduced temperatures when the system contracts and forms holes in the simulation box. As the system crystallizes, the pressure is strongly reduced. In the reheated system, the crystalline order is maintained and the pressure rises approximately linearly. The ''steps'' in the pressure curves with discontinuously reduced pressure are probably due to rearrangements in the crystal structure and partial closure of the holes in the system. At $T = 0.68$ the pressure jumps to the pressure of the cooled fluid system and the crystalline order is fully resolved. At the same point the orientational order vanishes. This happens in two distinct steps, reflecting the discontinuous behavior of the pressure. The orientational order can be mostly maintained as long as there is a strong positional order of the Janus spheres present in the system. Like the order parameters, the potential energy shows a pronounced hysteresis. The potential energy in the crystal is remarkably smaller than in the fluid phase. Unlike the pressure, the energy of the heated system shows no discontinuities apart from the step toward the fluid phase at $T = 0.68$.

3. Simulations at negative values of ε_3

The anisotropic, polar, and nematiclike phases discussed so far were obtained for systems made of ee Janus spheres and nn spheres with positive ε_1 respectively (cf. Table I. The discussion of Sec. IV has shown that no polar phase should

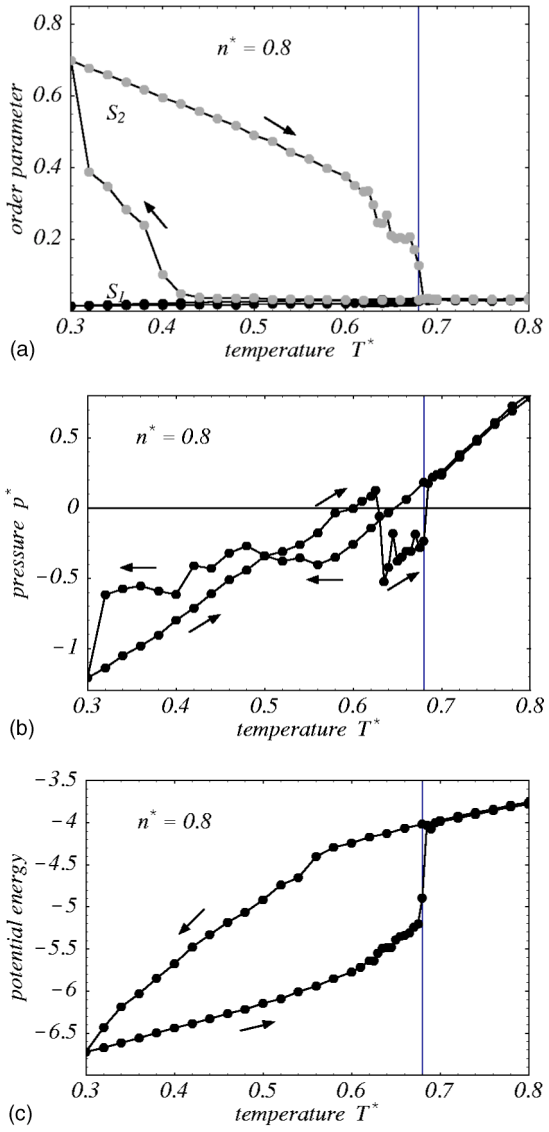

FIG. 17. Order parameters S_1 and S_2, the pressure, and the potential energy per particle of a Janus system with anisotropy parameters $\varepsilon_1=0.01$, $\varepsilon_2=-0.03$ and $\varepsilon_3=0$ as function of temperature. The number of Janus spheres is $N=1024$ and the average density is $n^*=0.8$. In each simulation the system was relaxed for 10^4 MC steps and the averages were extracted for 2×10^4 MC steps. In the range of the transition from the pseudonematic to the isotropic phase, the simulation time was increased afterward to improve the accuracy of the results and additional simulations were inserted at intermediate temperatures. The arrows mark the branches of the cooled and heated systems, respectively.

exist for $\varepsilon_1<0$. The MC simulations seem to confirm this finding. In simulations with nn Janus spheres with negative values for ε_1 and various choices for ε_2, no anisotropic behavior was observed above temperatures of $T=0.3$, when a simulation run was carried out as described above with a random initial configuration. However, in a simulation with a start configuration taken from the simulations of Fig. 17 at a temperature of $T=0.32$ of the cooled fluid, the alignment was maintained. But in this instance the system had already begun to crystallize and the final system was also crystalline, with a strong positional order.

VI. SUMMARY AND CONCLUSION

In this article we introduced a nonspherical model potential for Janus spheres (Sec. II), where two types of Janus spheres (nn and ee), with qualitatively different properties, were identified. A yet unobserved phase is predicted for the case of ee Janus spheres through an approximation for the free energy of the fluid, starting out from an augmented van der Waals approximation in Sec. III. All results presented in this article are expressed in dimensionless units Q^*, (see Sec. II). In order to predict the experimentally measurable analog Q based on our predictions, one needs an estimate for the diameter, mass, and LJ-type interaction strength between the Janus particles at hand, denoted in this article by r_0, m, and ϕ_0, respectively. Sample values were given in the Introduction.

An expression for the free energy f of the Janus fluid, suitable for a discussion on stability, was separated as follows: $f=f_{\mathrm{iso}}+f_{\mathrm{align}}$ with $f_{\mathrm{iso}}=f_{\mathrm{kin}}+f_{\mathrm{rep}}+f_{\mathrm{dis}}^{\mathrm{iso}}+f_{\mathrm{dis}}^{\mathrm{aniso}}$, and $f_{\mathrm{align}}=f_{\mathrm{dis}}^{\mathrm{align}}+f_{\mathrm{or}}$. All contributions are explicitly defined through Eqs. (5), (6),(8), and (10), together with the definitions for a number of virial coefficients provided by Eqs. (7), (11), and (12). These coefficients involve the model potentials given in Sec. II A. The corresponding expression for the pressure is given after Eq. (14). At this stage the free energy and the pressure depend on the single particle orientational distribution function $\rho(\mathbf{u})$ (or $\chi=4\pi\rho-1$) and three parameters $\varepsilon_{1,2,3}$ introduced in Eq. (4). The expressions were simplified by using a multipole expansion for χ. A further simplification invoked the assumption of uniaxial alignment (Sec. III D). Although it is possible to to evaluate the stated final expressions for the pressure, the order parameters, and the transition temperature (all in Sec. III) numerically, it is desirable to introduce another approximation which suffices to work out the influence of the anisotropy parameters $\varepsilon_{1,2,3}$ analytically. Results for the pressure of the fluid, the transition temperature into a polar phase and the order parameters in the polar phase were presented in Sec. IV by making use of a high temperature approximation. We presented a qualitative phase diagram and discussed the range of validity of — and possible corrections to — the analytical expressions. For the same model system Monte Carlo simulations were performed (Sec. V). Numerical results for the pressure, order parameters, and transition temperature were compared with the analytic results. The discussion (Sec. IV) has shown that no polar phase could exist for $\varepsilon_1<0$. The MC simulations seem to confirm this finding that actually no *liquid* anisotropic phase could be found in a system of Janus spheres with negative ε_1. Whereas analytically only a homogeneous polar phase is considered, in the simulations other anisotropic phases were also examined, namely, a nematiclike phase. Inhomogeneities and metastable (crystalline) states are observed in the simulation. These findings did not yet

enter the approximate analytical description of Janus fluids, but should motivate further studies. Furthermore, it is desirable to expand the anisotropic model potential from the description of spherical Janus particles to particles of nonspherical shape, e.g., ellipsoids. This can be achieved by insertion of higher order terms in the expansion (4) for the anisotropy function, in analogy with the description of nematic liquid crystals in Ref. [20].

ACKNOWLEDGMENTS

This work has been conducted under the auspices of the Sonderforschungsbereich SFB 448 ''Mesoskopisch strukturierte Verbundsysteme'' of the Deutsche Forschungsgemeinschaft (DFG). Financial support is gratefully acknowledged. We would like to thank Haiko Steuer, Martin Schoen, and Markus Antonietti for helpful discussions.

[1] C. Casagrande, P. Fabre, E. Raphaël, and M. Veyssie, Europhys. Lett. **9**, 251 (1989).
[2] R. Erhardt, A. Böker, H. Zettl, H. Kaya, W. Pyckhout-Heintzen, G. Krausch, V. Abetz, and A. H. E. Müller, Macromolecules **34**, 1069 (2001).
[3] S. Schrage (private communication).
[4] R. Erhardt, A. Böker, H. Zettl, H. Kaya, W. Pyckhout-Heintzen, G. Krausch, V. Abetz, and A. H. E. Müller, Polym. Mater. Sci. Eng. **84**, 102 (2001).
[5] J. N. Israelachvili, *Intermolecular and Surface Forces*, 2nd ed. (Academic Press, London, 1992).
[6] S. Hess, Physica A **267**, 58 (1999).
[7] S. Hess, in *Computational Physics*, edited by K. H. Hoffmann and M. Schreiber (Springer, Berlin, 1996) p. 268.
[8] S. Hess and M. Kröger, Phys. Rev. E **61**, 4629 (2000).
[9] J. E. Lennard-Jones, Physica (Amsterdam) **4**, 941 (1937)
[10] S. Hess and W. Köhler, *Formeln zur Tensor-Rechnung* (Palm and Enke, Erlangen, 1980).
[11] S. Hess, Z. Naturforsch. A **23a**, 597 (1968); Acta Phys. Austriaca, Suppl. **10**, 247 (1973).
[12] C. P. Borgmeyer, Diplomarbeit, Inst. füdur Theoretische Physik, Technische Universität Berlin, 1994.
[13] A. J. Stone, Mol. Phys. **36**, 241 (1978).
[14] J. Stelzer, R. Berardi, and C. Zannoni, Chem. Phys. Lett. **299**, 9 (1999); Mol. Cryst. Liq. Cryst. Sci. Technol., Sect. A **352**, 187 (2000).
[15] P. G. de Gennes and J. Prost, *The Physics of Liquid Crystals* (Oxford University Press, Oxford, 1993).
[16] J. P. Hansen and I. R. MacDonald, *Theory of Simple Liquids* (Academic Press, London, 1976).
[17] J. D. Weeks, D. Chandler, and H. C. Andersen, J. Chem. Phys. **54**, 5237 (1971).
[18] F. Carnahan and K. Starling, J. Chem. Phys. **51**, 635 (1969).
[19] S. Hess, M. Kröger, and H. Voigt, Physica A **250**, 58 (1998).
[20] S. Hess and Bin Su, Z. Naturforsch A: Phys. Sci. **54**, 559 (1999).
[21] W. Maier and A. Saupe, Z. Naturforsch. A **14A**, 882 (1959); *ibid.* **15A**, 287 (1960).
[22] S. Hess and M. Kröger, Phys. Rev. E **64**, 011201 (2001).
[23] M. P. Allen and D. J. Tildesley, *Computer Simulation of Liquids* (Clarendon, Oxford, 1987).
[24] N. Metropolis, A. W. Rosenbluth, M. N. Rosenbluth, A. H. Teller, and E. Teller, J. Chem. Phys. **21**, 1087 (1953).
[25] D. P. Landau and K. Binder, *A Guide to Monte Carlo Simulations in Statistical Physics* (Cambridge University Press, Cambridge, England, 2000).
[26] M. J. H. Hagen, E. J. Meijer, G. C. A. M. Mooij, D. Frenkel, and H. N. W. Lekkerkerker, Nature (London) **365**, 425 (1993).